



HAL
open science

A slitless spectroscopic survey for H α emission-line objects in SMC clusters

Christophe Martayan, Dietrich Baade, Juan Fabregat

► **To cite this version:**

Christophe Martayan, Dietrich Baade, Juan Fabregat. A slitless spectroscopic survey for H α emission-line objects in SMC clusters. *Astronomy & Astrophysics - A&A*, 2010, 509, pp.11. 10.1051/0004-6361/200911672 . hal-03742802

HAL Id: hal-03742802

<https://hal.science/hal-03742802v1>

Submitted on 5 Sep 2022

HAL is a multi-disciplinary open access archive for the deposit and dissemination of scientific research documents, whether they are published or not. The documents may come from teaching and research institutions in France or abroad, or from public or private research centers.

L'archive ouverte pluridisciplinaire **HAL**, est destinée au dépôt et à la diffusion de documents scientifiques de niveau recherche, publiés ou non, émanant des établissements d'enseignement et de recherche français ou étrangers, des laboratoires publics ou privés.

A slitless spectroscopic survey for H α emission-line objects in SMC clusters[★]

C. Martayan^{1,2}, D. Baade³, and J. Fabregat⁴

¹ European Organisation for Astronomical Research in the Southern Hemisphere, Alonso de Cordova 3107, Vitacura, Casilla 19001, Santiago 19, Chile

e-mail: Christophe.Martayan@eso.org

² GEPI, Observatoire de Paris, CNRS, Université Paris Diderot, 5 place Jules Janssen, 92195 Meudon Cedex, France

³ European Organisation for Astronomical Research in the Southern Hemisphere, Karl-Schwarzschild-Str. 2, 85748 Garching b. München, Germany

⁴ Observatorio Astronómico de Valencia, edifici Instituts d'investigació, Poligon la Coma, 46980 Paterna Valencia, Spain

Received 16 January 2009 / Accepted 2 September 2009

ABSTRACT

Context. A fair fraction of all single early-type stars display emission lines well before their supergiant phase. Very rapid rotation is necessary for these stars to form rotationally supported decretion disks. However, it is unknown whether and which other parameters may be important.

Aims. We assess the roles of metallicity and evolutionary age in the appearance of the so-called Be phenomenon.

Methods. Slitless CCD spectra were obtained covering the bulk (about 3 square degrees) of the Small Magellanic Cloud. For H α line-emission twice as strong as the ambient continuum, the survey is complete to spectral type B2/B3 on the main sequence. About 8120 spectra of 4437 stars were searched for emission lines in 84 open clusters, and 370 emission-line stars were found, among them at least 231 close to the main sequence. For 176 of them, photometry is available from the OGLE database. For comparison with a higher-metallicity environment, the Galactic sample of the photometric H α survey by McSwain & Gies (2005, ApJS, 161, 118) was used.

Results. Among early spectral sub-types, Be stars are more frequent by a factor ~ 3 –5 in the SMC than in the Galaxy. The distribution with spectral type is similar in both galaxies, i.e., not strongly dependent on metallicity. The fraction of Be stars does not seem to vary with local star density. The Be phenomenon mainly sets in towards the end of the main-sequence evolution (this trend *may* be more pronounced in the SMC); but some Be stars already form with Be-star characteristics. In small subsamples (such as single clusters), even if they appear identical, the fraction of emission-line stars can deviate drastically from the mean.

Conclusions. In all probability, the fractional critical angular rotation rate, Ω/Ω_c , is one of the main parameters governing the occurrence of the Be phenomenon. If the Be character is only acquired during the course of evolution, the key circumstance is the evolution of Ω/Ω_c , which is not only dependent on metallicity but differently so for different mass ranges. As a result, even if the Be phenomenon is driven basically by a single parameter (namely Ω/Ω_c), it can assume a complex multi-parametric appearance. The large cluster-to-cluster differences, which seem stronger than all other variations, serve as a caveat that this big picture may undergo significant second-order modulations (e.g., pulsations, initial angular momentum, etc.).

Key words. stars: early-type – stars: emission-line, Be – stars: fundamental parameters – stars: evolution – magellanic clouds – catalogs

1. Introduction

The so-called Be phenomenon manifests itself in terms of a single, intermittent, or permanent occurrence of emission lines in main-sequence stars with spectral types between O and A. This line emission arises from rotationally supported disks formed by matter lost (often ejected) by the central star. An excellent introduction to the complex idiosyncrasies of Be stars is given by Porter & Rivinius (2003). While extremely rapid rotation is a necessary condition for the Be phenomenon, it is not clear whether it is also sufficient or which other conditions need to be fulfilled. There are reports suggesting that the Be phenomenon also depends on metallicity (Maeder et al. 1999) and

evolutionary phase (e.g., Fabregat & Torrejón 2000; Martayan et al. 2007b). An obvious method for investigating the latter possibility is the study of open star clusters with a suitable range of ages. In the Galaxy, this has been applied various times but mostly using photometric techniques. A very good discussion of the subject and previous work can be found in McSwain & Gies (2005).

In the Small Magellanic Cloud (SMC), a major spectroscopic survey for emission-line objects was performed by Meyssonnier & Azzopardi (1993). Although it identified 1898 emission-line objects, the photographic nature of the data did not permit many emission-line stars to be found that were close to the main sequence or in crowded areas such as open clusters. This paper reports on the first digital slitless spectroscopy survey of the SMC in search of Oe/Be/Ae stars (a second paper will concern the LMC). During its execution, some 3 million spectra were obtained.

[★] Tables A.1, A.2, B.1, B.2, C.1–C9 is only available in electronic form at the CDS via anonymous ftp to [cdsarc.u-strasbg.fr](ftp://cdsarc.u-strasbg.fr) (130.79.128.5) or via <http://cdsweb.u-strasbg.fr/cgi-bin/qcat?J/A+A/509/A11>

2. Observations

The observations¹ were carried out (by JF) on September 25 and 26, 2002 with the Wide Field Imager (WFI) attached to the 2.2 m MPG Telescope at ESO's observatory on Cerro La Silla in Chile (see Baade et al. 1999). Because of bad weather, the second night was only partly useful.

In its slitless spectroscopic mode, the WFI has a roughly circular field of view of diameter 0.31 degrees. The R50 grism yields a dispersion of 54 nm/mm or 0.811 nm/pixel. The nominal resolution at optimal focus and seeing is 5.1 nm at H α . To reduce crowding and overlapping spectra, the lengths of the spectra were limited by means of a filter with a full-width-at-half-maximum of 7.4 nm centred on H α . This means that spectra are acceptably separated if the stars are 2'' apart perpendicular to the dispersion direction and 6'' apart along this direction. These numbers vary slightly with the quality of the focus. But in general they do not require an adaptation of the parameters for the automatic extraction by software of the spectra.

The exposure time per field was set to 600 s. The coverage of the SMC achieved with 14 telescope pointings is shown in Fig. 1.

For a similar study with the WFI but in the Galaxy and with a broader filter, see Martayan et al. (2008).

3. Data reduction, extraction of spectra, and identification of emission-line stars

3.1. Data reduction

The elementary CCD image processing was performed with IRAF² tasks and the MSCRED package.

The subsequent extraction of the bias- and flat field-corrected spectra posed considerable technical challenges:

- all images suffer from substantial and non-homogeneous defocus, which increases from the field center to the edges. The reasons could not be reconstructed. However, special developed techniques permit continuum and emission-line objects to be distinguished at a fairly acceptable level of confidence, turning the problem almost into an advantage (see Fig. 2);
- each object appears in several spectral orders. The 0th order is undispersed and corresponds to the point spread function (PSF). The order suitable for extraction of the H α spectra is -1 , which in the following is referred to as “the spectrum”. In the case of bright stars, up to 7 or even 8 orders are visible, significantly increasing the probability of spectra being contaminated. While this implies the possible non-detection of some emission-line objects, it will not lead to false detections because even the 0th order has a very different PSF;
- there are parasitic spectra resulting from scattered light from stars outside the direct field of view;
- the position angle of the dispersion direction varies (by $\leq \pm 5^\circ$) from the center to the edges of the images.

In principle, spurious detections of emission-line objects may arise from particle events or hot pixels. However, their very different PSFs ensure that these confusions are rather unlikely. The extraction algorithm used tries to automatically reject particle

hits. On the other hand, the completeness of the survey is reduced by spectra falling onto the gaps (amounting to 3.1% in area) between the 4×2 CCDs of the WFI.

After careful, realistic tests with representative subsets of the data, it was decided that it is not just most time effective but also more reliable to allow properly tuned software to search for spectra automatically. For this task and the 2-D extraction of the spectra, SExtractor (Bertin & Arnouts 1996) was employed with specially adapted convolution masks (Bertin, private communication). About 3 million spectra were extracted across the entire SMC (14 images, see Fig. 1), of which about 1 million are useful.

A comparison of these extracted spectra with spectra extracted by eye suggests that the extraction efficiency in clusters is on average around 75 to 80%, depending on the area density of the stars. With position of the cluster in the WFI field, i.e., mainly the level of defocus, this mean value may range from 60% to 100%.

Because of the need to work on samples with defined ages, only the areas of 83 clusters listed in the OGLE database (Udalski et al. 1998) and a number of neighboring comparison fields (14 fields, 1 or 2 per target field and with diameters of 2 to 4', located close to the open clusters treated) were retained for the classification of stars with and without line emission. The open clusters selected in this way (from Pietrzynski & Udalski 1999) are compiled in Table B.1; other parameters (e.g., total number of stars, number of emission-line stars) are included (where applicable, separately for multiple observations of a given cluster). This process yielded to a sample of 7867 spectra for examination for the presence of line emission.

The WFI database includes an 84th open cluster, NGC 346, which is a complex young structure, probably consisting of a number of subaggregates. However, OGLE-2 photometry is not available for this dense field, which is affected by extended nebular emission. Details are given in Sect. A. Figure 3 shows the distribution of studied open clusters in the SMC, as well as the metallicity areas by Cioni et al. (2006). They confirm that the open clusters are in metallicities significantly lower than those of Galactic open clusters.

3.2. Identification of emission-line stars: the Album code

The exploratory tests alluded to above also showed that the software was unable to reliably distinguish without human interaction, between stars with and without H α line emission. However, the visual classification of several thousand spectra would be facilitated greatly by transforming them into an easy-to-classify format. To this effect, the *Album* package was written (in IDL).

Album starts out from the assumption that the 2-D PSF varies only slowly with position in the frame. To compute the 2-D PSF, typically 50–250 spectra were registered (by cross-correlation), coadded, and normalized. This step is operator-supervised; and unsuitable stars can be rejected. In the first step, all obvious emission-line stars, apparent binaries, too closely spaced sources, spectra with severe particle hits or otherwise reduced quality are rejected and a new regional mean spectrum is computed. It was empirically established that the inclusion, at the $\leq 5\%$ level, of emission-line objects only insignificantly modifies the regional mean spectrum profile. The resulting regional template spectrum was subtracted (after cross-correlation and shift in X and Y) from each normalized 2-D spectrum (see Fig. 2-left) to be checked for H α line emission. *Album* also automatically rejects artifacts such as ghosts or particle events by applying a suite of tests to the shapes of the spectra.

¹ Observations at the European Southern Observatory, Chile under project number 069.D-0275(A).

² IRAF is distributed by the US National Optical Astronomy Observatory, which is operated by the Association of Universities for Research in Astronomy (AURA), Inc., under cooperative agreement with the US National Science Foundation.

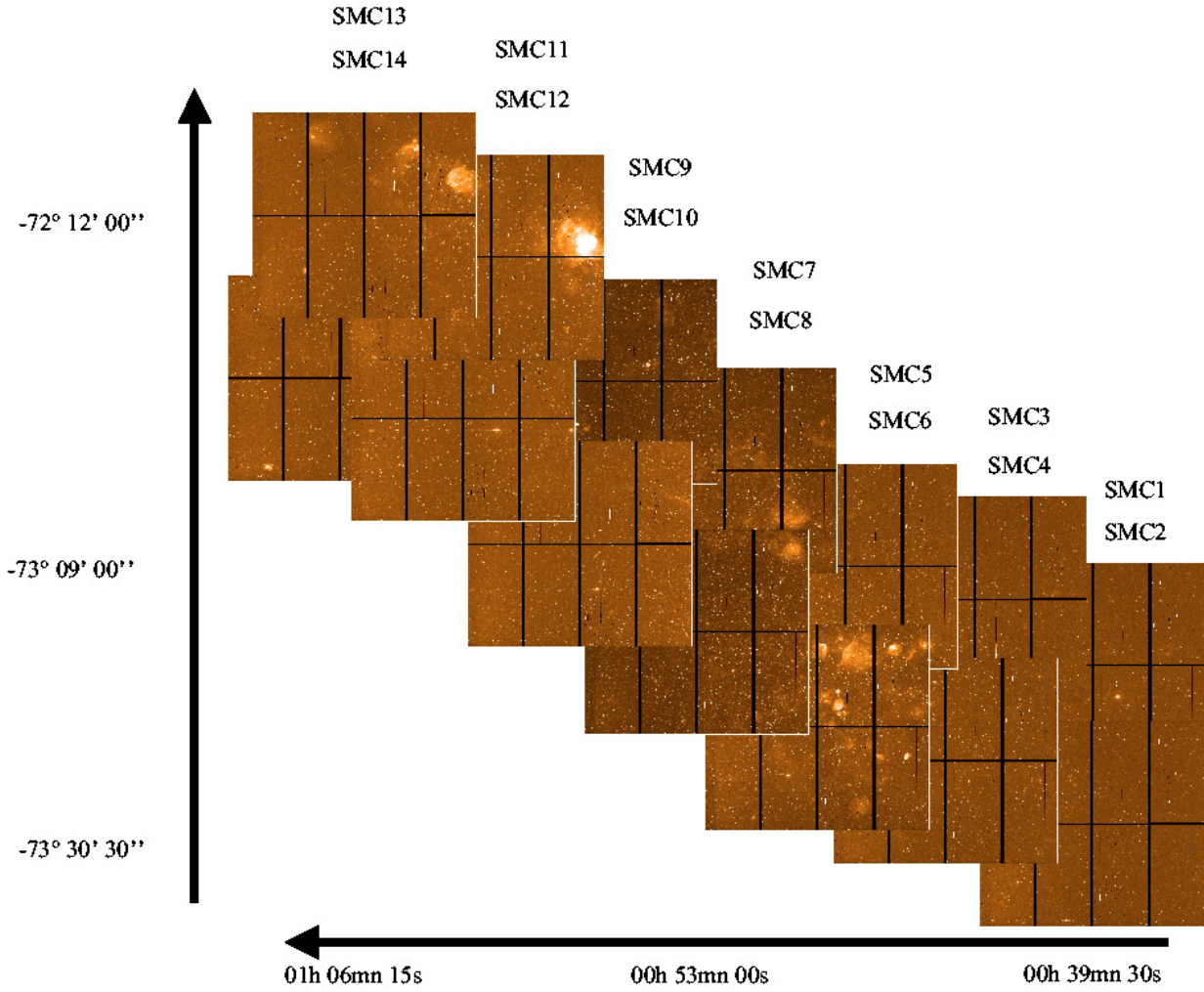


Fig. 1. The tiling by WFI frames of the Small Magellanic Cloud.

In the case of emission-line stars, the 2-D spectra exhibit a secondary peak (see Fig. 2). However, after subtraction of the mean PSF the resulting difference images display a more characteristic and conspicuous ring-like structure. This is because of the large defocus, which affects at most marginally resolved line emission such as that of a point source. Therefore, while the continuum flux is just blurred by the defocus, the line emission takes on roughly the shape of a doughnut or horseshoe (i.e., the telescope pupil).

In a properly prepared and homogeneous album (hence the name *Album*) of images, this peculiar structure is more readily and reliably identified by the human eye than by software developed with the same amount of effort.

Using this scheme, all stars were classified into three categories: definite emission-line stars, candidate emission-line stars, and stars without $H\alpha$ line emission. An emission-line star is considered to be definite, if its flux distribution shows a significant secondary peak (cf. Fig. 2) at a position consistent with $H\alpha$. Obviously, this depends on the signal-to-noise ratio but also on the location within the frame and the associated defocus. If the purity of this signature is potentially diluted by particle events or noise spikes, the object is called a candidate emission-line star. For example, for relatively bright objects in the range $V = 14$ to 17, between 100% and 80% of the emission-line stars found are classified as definite emission-line stars. However, towards

lower brightness and lower signal-to-noise ratio, the fraction of definite emission-line stars declines to between 55 and 13%.

3.3. Efficiency of $H\alpha$ emission detection

To determine the thresholds for the detection of $H\alpha$ emission, *Album* was applied to WFI observations of the open cluster NGC 330 and its well-studied population of Be stars. With the help of *SIMBAD*, the previously known Be stars and those found by *Album* were compared, and the $H\alpha$ equivalent widths and line strengths were taken from Hummel et al. (1999, 2001); Martayan et al. (2007a), which were similar to the WFI observations of NGC 6611 by Martayan et al. (2008). The results are shown in Fig. 4 for the detection efficiency in terms of $H\alpha$ line-emission equivalent width (top) and strength (bottom). The *Album*-based procedure found slightly less than 80% of the Be stars known in NGC 330.

Figure 4 suggests that our SMC survey technique detects $H\alpha$ line emission, when the equivalent width is higher than 10 \AA , or the peak intensity is more than twice that of the underlying continuum, down to $V \sim 16.5\text{--}17$ mag, which corresponds to spectral types later than B2-B3 (see Martayan et al. 2007b). We note that, in contrast to the conventional definition, positive values indicate a net line emission. For fainter stars, the signal-to-noise ratio is lower and the detection threshold increases.

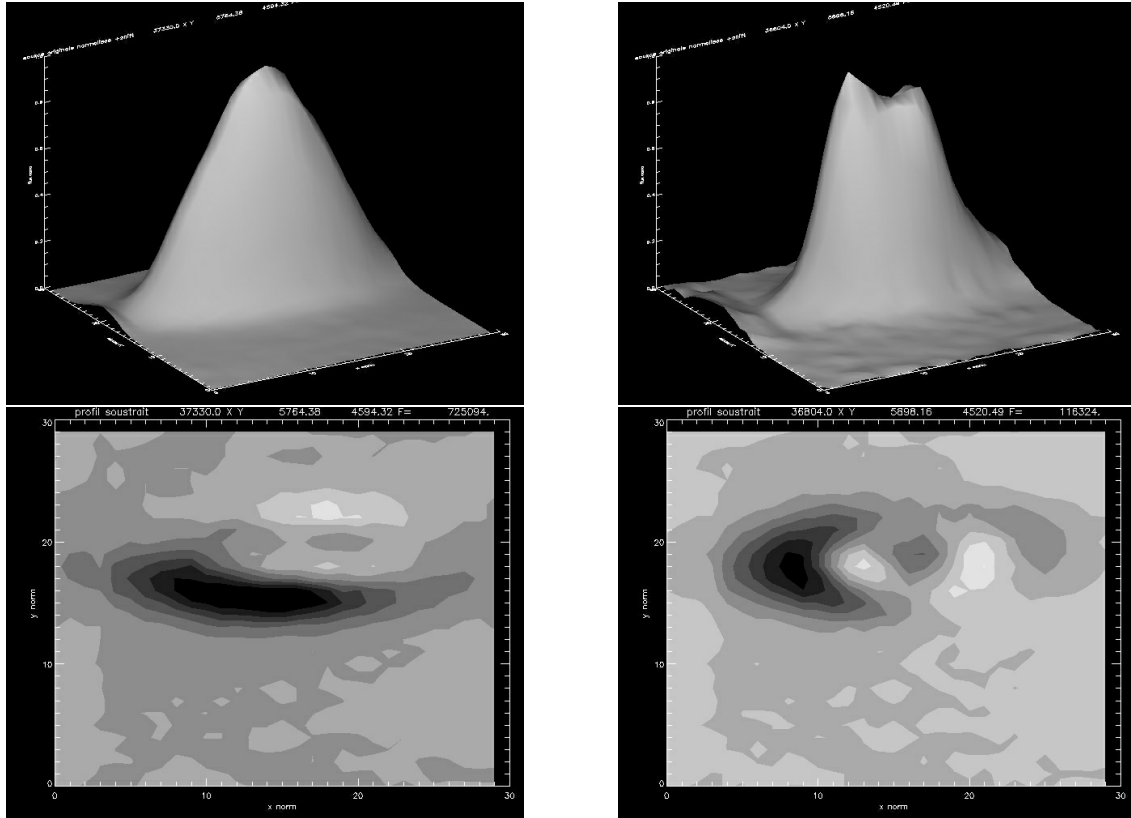


Fig. 2. The appearance of objects with and without $H\alpha$ line emission in defocused slitless WFI spectra. *Left*: non-emission-line star, *right*: emission-line star. *Top*: 3-D presentations of the original flux distributions, *bottom*: 2-D projections of the residuals after subtraction of the mean, scaled point spread function (PSF) of pure continuum sources. While a pure continuum source is just blurred by the defocus, a (nearly unresolved) emission line is effectively imaged like a point source, yielding a roughly donut (or horseshoe) like image of the pupil. The bright excess above the mean of the image corresponding to the emission peak is visible in the middle-left of the horseshoe (*bottom right* figure).

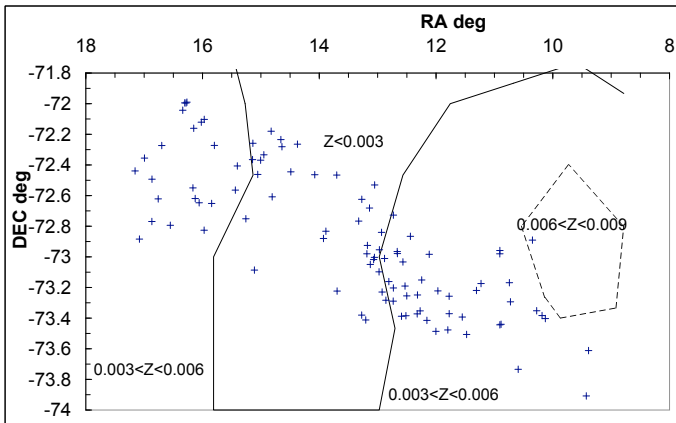


Fig. 3. The positions of the WFI SMC clusters superimposed on spatial isometallicity curves (from Cioni et al. 2006).

A further check was made in the following way: Martayan et al. (2007b) observed 31 WFI stars preselected from the emission-line stars found with the WFI in the field of NGC 330. At a spectral resolving power of 8600 with the VLT, all of the 31 emission-line stars were confirmed as true $H\alpha$ emission-line objects, 28 of which could be classified as Be stars. The remaining 3 turned out to be of a different nature (compact planetary nebulae, supergiants, B[e], or Herbig B[e] stars).

The case of NGC 330 is also useful for guessing the false-alarm probability, which is evidently low. For a more precise

constraint, one would need to have a control sample with B/Be classifications that are accurate at the time of the WFI observations. This does not exist, and some instrument-independent uncertainty is introduced by the comparison of observations made in different years because the Oe/Be/Ae characteristics of a star are (sometimes: highly) time-dependent and quite often present only intermittently.

4. Astrometry, photometry, and spectral classification

For the detected emission-line stars to be placed in an evolutionary context, intrinsic colours and magnitudes are needed. In the following subsections, these are derived separately for both the WFI emission-line stars in the SMC and a comparison data set in the Galaxy.

4.1. WFI SMC data

As the largest homogeneous source of photometry in SMC clusters, we chose OGLE (Udalski et al. 1998). The first step in the cross-identification is astrometry.

4.1.1. Astrometry and correlation with OGLE

The ASTROM package (Wallace & Gray 2003) was applied to the extracted spectra of the -1st order. Within each WFI image, 30 to 80 astrometric reference stars from the GSC2.2

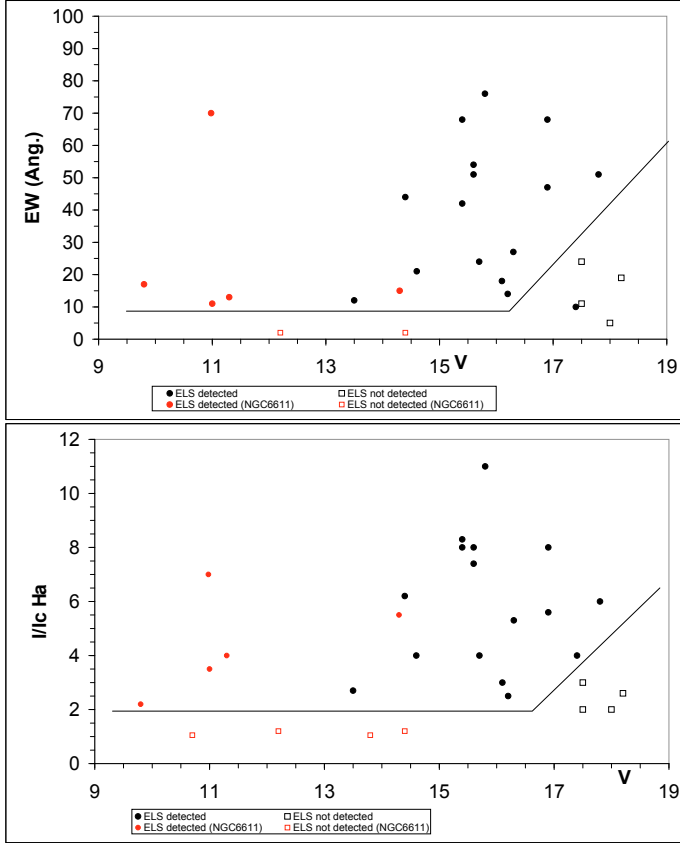


Fig. 4. Detection efficiency in equivalent width (*top*) and peak line strength relative to the continuum (*bottom*) of H α emission with WFI slitless spectra. The H α data are from Hummel et al. (1999, 2001) and Martayan et al. (2007a, 2008) for NGC 330 (black) and NGC 6611 (red). Emission-line stars detected in the WFI data are represented by filled circles, open squares denote the misses. Note that, contrary to the conventional definition, positive values indicate a net line emission.

and/or UCAC2, USNO catalogues were utilized. In this way, the coordinates of the 7,867 SMC stars mentioned in Sect. 3.1 (plus 55 in NGC 346) were determined with an accuracy of 0.5–1". Cross-correlating these WFI positions with the OGLE catalogues (Udalski et al. 1998) revealed a systematic global offset of $-0.3''$ in right ascension and $+0.3''$ in declination. To maximize the probability of identifying the WFI emission-line stars in OGLE, these shifts were applied to the photometric data extracted from OGLE (note that the WFI coordinates provided in this paper do not include these offsets).

For each cluster, any multiple observations and identifications were merged into one per star. Table B.2 provides a summary of the results for each cluster. On average, 73.7% of all WFI stars and 79.7% of the WFI emission-line stars were found in OGLE. The incompleteness is caused by that of OGLE-2, which is incomplete in crowded areas (i.e., clusters) and in the presence of extended nebulosities. However, imperfect WFI coordinates are also a contributing factor. We note also that only about 80% of the ~ 3 square degrees of this WFI survey are covered by OGLE-2. This especially affects large complexes such as that of NGC 346.

4.1.2. Photometric spectral classification

The resulting apparent colours and magnitudes need to be converted into absolute values, and absolute luminosities and

Table 1. Calibration used for the classification of the star¹.

ST	Mv Range	ST	Mv Range
Hot O	< -6.0	B6	$[-0.6; -0.25[$
O3	$[-6.0; -5.9[$	B7	$[-0.25; 0.025[$
O4	$[-5.9; -5.7[$	B8	$[0.025; 0.285[$
O5	$[-5.7; -5.5[$	B9	$[0.285; 0.43[$
O6	$[-5.5; -5.2[$	A0	$]0.43; 1.0[$
O7	$[-5.2; -4.9[$	A1	$[1.0; 1.3[$
O8	$[-4.9; -4.5[$	A2	$[1.3; 1.5[$
O9	$[-4.5; -4.2[$	A3-A4	$[1.5; 1.95[$
B0	$[-4.2; -3.25[$	A5-A6	$[1.95; 2.2[$
B1	$[-3.25; -2.55[$	A7	$[2.2; 2.4[$
B2	$[-2.55; -1.8[$	A8-A9	$[2.4; 2.55[$
B3	$[-1.8; -1.4[$	F0-F1	$[2.55; 3.6[$
B4	$[-1.4; -0.95[$	cool F	≥ 3.6
B5	$[-0.95; -0.6[$		

¹The classification is based on ranges in absolute V magnitude per spectral sub-type, following the calibration of Lang (1992) and Wisniewski & Bjorkman (2006, and references therein) for main-sequence stars.

spectral types need to be derived so that intercluster comparisons within the SMC and also between SMC and Galaxy become possible. The parameters V_0 , $(B - V)_0$, $(V - I)_0$ were derived by means of the per-cluster E_{B-V} reddenings from Pietrzynski & Udalski (1999). The absolute M_V of each star was calculated from the resulting V_0 and the SMC distance modulus provided by Udalski (2000). That is, for all clusters the same effective distance was adopted.

Using the HR diagram in Fig. 5, the following regions were assumed to delineate the main sequence:

- O stars: $M_V < -4.2$ and $-0.3 \leq (B - V)_0 \leq +0.1$ and $-0.3 \leq (V - I)_0 \leq +0.3$;
- B stars: $-4.2 \leq M_V \leq +0.43$ and $-0.4 \leq (B - V)_0 \leq +0.1$ and $-0.35 \leq (V - I)_0 \leq +0.2$;
- A stars: $0.43 < M_V \leq 2.55$ and $-0.4 \leq (B - V)_0 \leq +0.25$ and $-0.38 \leq (V - I)_0 \leq +0.25$.

Individual spectral types were assigned by applying the calibration of Lang (1992) and Wisniewski & Bjorkman (2006, and references therein) as shown in Table 1 and Fig. 5. The breakdown of the full sample in terms of spectral types and emission-line characteristics is given in Table 2.

Apart from the global uncertainties in spectral types derived from photometry, differential reddening across a cluster and erroneous membership assignments will introduce individual errors. However, they will only dilute but not probably falsify general trends derived from the database at large.

Section A.3 compares for 12 stars in NGC 346 spectral types derived as described above and spectroscopic classifications from the literature. The average difference amounts to only 1 spectral subtype.

The results of the photometric and spectral classification and additional information are compiled in a number of tables. For basic data of Be stars and their absolute photometric data and spectral types, we refer to Tables C.1 and C.2, respectively. For only candidate-Be stars, Tables C.3 and C.4 provide the equivalent data. Tables C.5 and C.6 concern Oe and Ae stars. Emission-line objects well outside the main sequence are covered in Tables C.7 and C.8. Table C.9 compiles all WFI-based data (coordinates, etc.) of emission-line stars without a counterpart in the OGLE catalogues (Udalski et al. 1998). Where

Table 2. Breakdown of WFI SMC sample (Col. 2) and the Galactic sample (Col. 3)¹.

Type	Number (SMC)	Number (Galaxy)
Open clusters	84	54
O	25	13
Oe+Oe?	6	3
B	1384	1741
Be	109	52
Be?	54	116
A	250	495
Ae+Ae?	7	57
Other non-ELS	2408	17 845
ELS outside main sequence	90	
Unclassified ELS	49	
NGC 346 (Be, HBe, WR, etc.)	55	
Total	4437	20 322

¹ The Galactic sample is from [McSwain & Gies \(2005\)](#) (Col. 3). The number of stars per spectral types, and per emission-line characteristics are given. ELS denotes emission-line stars. The first line after the titles gives the number of open clusters used.

applicable, the tables also contain information extracted from SIMBAD within a search radius of 2'' about each emission-line star. Because of the high density of objects especially in the cluster cores, this information will inevitably suffer from misidentifications.

Similar tables for the 3792 SMC non-emission line stars are available on request.

4.2. Comparison data for the Galaxy

The most recent and comprehensive photometric survey of Be stars in Galactic clusters to date is that of [McSwain & Gies \(2005\)](#). It comprises 52 definite Be stars and 116 Be candidates in 48 of the 54 clusters studied. Using data from [McSwain et al. \(2008\)](#), we estimate that the detection limit for H α line emission in that sample is 7 Å, similar to that of our spectroscopic study in the SMC.

[McSwain & Gies \(2005\)](#) published the Stroemgren parameters y , $(b - y)$, $E(b - y)$ but not m_1 . For a comparison with the SMC sample, the conversion to the Johnson UBV system was performed as follows:

- first, $(B - V)$ was derived from the relation [Warren & Hesser \(1977\)](#): $(B - V) = 1.668 \times (b - y) - 0.030$;
- second, the y magnitudes given by [McSwain & Gies \(2005\)](#) in the system defined by [Cousins \(1987\)](#) were transformed into standard V magnitudes by means of the relation $V = y + 0.038 \times (B - V)$ ([Cousins & Caldwell 1985](#));
- third, $E[B - V]$ was derived from $E[B - V] = E[b - y]/0.745$, where $E[b - y]$ is taken from [McSwain & Gies \(2005\)](#);
- fourth, V_0 was obtained from $V_0 = V - 3.1 \times E[B - V]$;
- fifth, absolute magnitudes, M_V , were calculated from $M_V = V_0 - \mu$, using the distance moduli, μ , given by [McSwain & Gies \(2005\)](#) for each cluster;
- sixth, $(B - V)_0 = (B - V) - E[B - V]$.

From this point on, spectral types of main-sequence stars were derived in the same way as for the WFI SMC sample (Sect. 4.1.2).

5. Results and discussion

5.1. Topology of global HR diagrams

Reddening-free colour–magnitude diagrams incorporating all the WFI stars in the SMC clusters are shown in Fig. 5. Emission-line stars are either found on or close to the main sequence, the red giant branch, and the asymptotic giant branch. As expected from Fig. 4, the number of stars seems to become visibly incomplete below $V = 17$ mag (corresponding to $M_V \simeq -2.1$).

The emission-line stars close to the main sequence are mainly Be stars. While their spread in colour is not larger than that the apparent zero-age main sequence, they are displaced significantly towards redder colours. This topology is discussed in more detail in Sect. 5.2. An analogous diagram (M_V vs. $(B - V)_0$) of the Galactic data from [McSwain & Gies \(2005\)](#) is depicted in Fig. 6. For all open SMC clusters with emission-line stars and data for a total of at least 10 stars, separate colour–magnitude diagrams are also available (see Figs. D.1 to D.8 in Sect. D).

5.2. Colour excesses of emission-line stars

Table 3 contains the mean colour offset per spectral subtype between emission and non-emission line stars (separately for SMC and Galaxy). Not only are emission-line stars redder than non-emission line stars but they may even possibly delineate a separate red sequence. This is already on average more prominent in $(V - I)_0$ than in $(B - V)_0$ but some individual stars deviate much more strongly in $(V - I)$ than in $(B - V)$. In $(B - V)$, the Galactic Be stars seem to deviate more strongly from the normal main sequence than in the SMC. Since for early-type stars the colour–magnitude diagrams are degenerate in colour, nothing can be said about any systematic differences in luminosity.

The excess reddening seems to reach a maximum around spectral types B0-B2 in both SMC and Galaxy. Figures 7 and 8 illustrate the reddening excess between emission and non-emission line stars in $(B - V)_0$ and $(V - I)_0$ in the SMC and Galaxy. Similar segregations of Be and normal B stars were also found by [Keller et al. \(1999\)](#). This could be due to one or more of stellar evolution, light scattering in the circumstellar disk ([Dachs et al. 1988](#)), and gravitational darkening linked to the rapid rotation of Be stars ([Frémat et al. 2005](#)). Of these, evolutionary differences are the least likely since the comparisons are made for stars in the same open clusters and of similar spectral type. (The evolutionary status is discussed in more detail in Sect. 5.6.)

This leaves rapid rotation and circumstellar disks as candidate explanations of the extra reddening in Be stars. At low metallicity (SMC), Be stars seem to rotate faster than at high metallicity ([Martayan et al. 2007b](#)), so it is expected that the rapid rotation effects are larger in the SMC than in the Galaxy. In theory ([Maeder & Meynet 2001](#)), this is partly compensated by the radii of low-metallicity stars being smaller by between 15 and 20%, which can affect the luminosity of the stars. On the other hand, work by [Trundle et al. \(2007\)](#) and [Evans et al. \(2008\)](#), indicates that, in the SMC, the class V stars of a given spectral subtype are hotter than their counterparts in the Galaxy. However, their luminosity is about the same: for B0V, $L_{\text{SMC}}/L_{\text{MW}} = 0.9$; for B1V, $L_{\text{SMC}}/L_{\text{MW}} = 1.01$; for B2V, $L_{\text{SMC}}/L_{\text{MW}} = 1.04$.

Circumstellar disks of Be stars have been reported ([Wisniewski & Bjorkman 2006](#); [Wisniewski et al. 2007a](#); [Martayan et al. 2007a](#)) to be closer to the central star at lower metallicity, so that the circumstellar extinction towards low-inclination Be stars would be increased. However, as explained

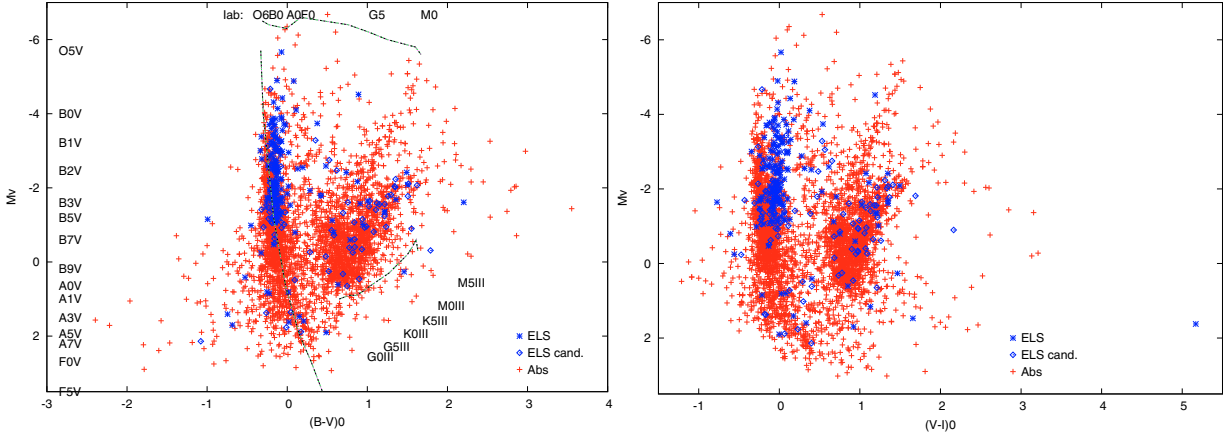


Fig. 5. Global colour–magnitude diagrams for stars in SMC open clusters. *Left:* $B - V$; *right:* $V - I$, absolute V magnitude versus (hereafter vs.) dereddened colour. Red crosses (+) indicate non-emission line stars, blue asterisks (*) mark emission-line stars (“ELS”), and candidate emission-line stars (“ELS cand.”) are plotted as diamonds. The spectral calibration sequences represented by the lines displayed in the figure are taken from Lang (1992).

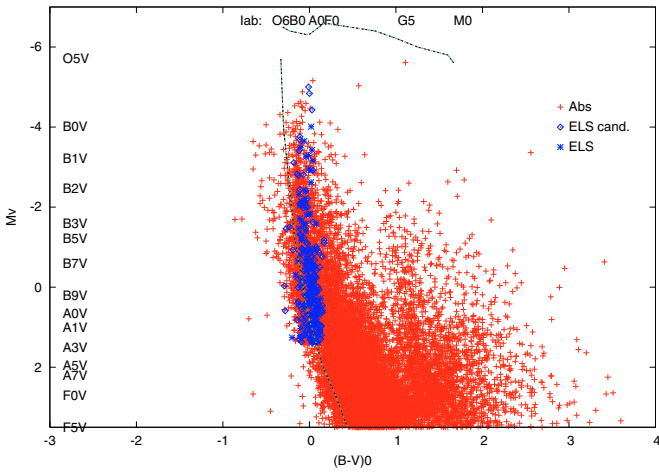


Fig. 6. Global absolute V magnitude vs. dereddened $(B - V)_0$ colour of the Galactic open cluster stars from McSwain & Gies (2005). The spectral calibration sequences corresponding to the lines displayed in the figure are from Lang (1992). The symbols are the same as in Fig. 5.

above, the radii of the stars are smaller, thereby partly offsetting the claimed difference in geometry.

5.3. Frequency of Be stars as a function of local star density

Various studies in the Galaxy (for example Keller 2004) suggest that the rotational velocities of B stars are higher in open clusters than in the field. In contrast, investigations in both the LMC and SMC using statistical tests (Martayan et al. 2006, 2007b) did not find significantly different rotational velocities in clusters and the field. In the Galaxy, Huang & Gies (2006) found a larger number of slow rotators in the field than in open clusters. They also concluded that the more massive B stars spin down during their main-sequence phase and suggested that some of the rapid rotators found may have been spun up by mass-transfer in close binary systems. These authors ascribe the difference in velocity between open clusters and fields to a difference in the evolutionary phase of the stars (the older the stars are, the slower they are).

The same difference is attributed by Wolff et al. (2007) to the difference in number density. They argue that stars in

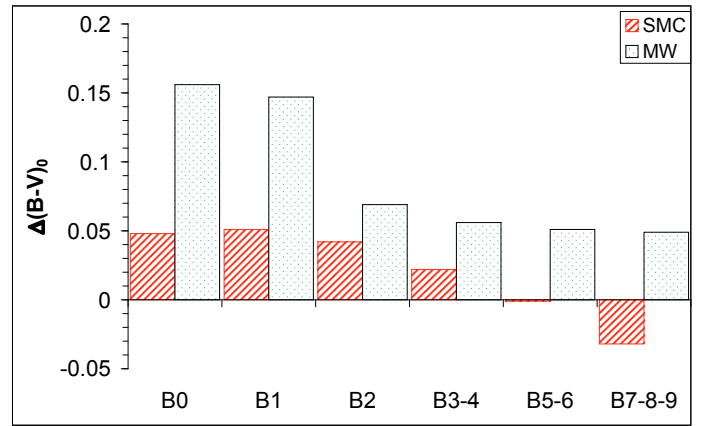


Fig. 7. Comparison between normal stars and emission-line star of the reddening excess in $(B - V)_0$ in the SMC (*left*) and Galaxy (*right*, from data of McSwain & Gies 2005). Note that the sample is not complete starting with spectral type B3.

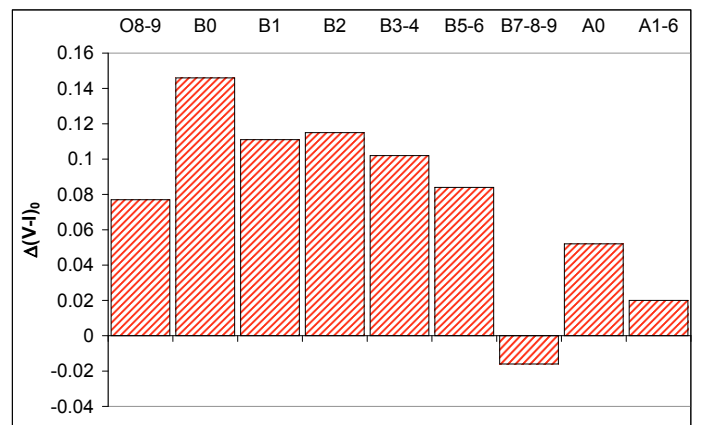


Fig. 8. Comparison between normal stars and emission-line star of the reddening excess in $(V - I)_0$ in the SMC.

low-density environments could retain their pre-main sequence disk for a longer time. Star-disk locking would then preserve the angular speed, preventing these stars from becoming young rapid rotators.

Table 3. Average magnitude and colour index values per spectral type categories of normal and emission-line stars¹.

ST	M_V	$(B - V)_0$	$\Delta(B - V)_0$	$(V - I)_0$	$\Delta(V - I)_0$	N	Galaxy $(B - V)_0$	Galaxy $\Delta(B - V)_0$
O8-O9	-4.522	-0.123		-0.063		16	-0.227	
O8-O9e	-4.638	-0.098	0.025	0.014	0.077	5		
B0	-3.569	-0.190		-0.154		49	-0.286	
B0e	-3.569	-0.142	0.048	-0.008	0.146	27	-0.130	0.156
B1	-2.781	-0.211		-0.177		90	-0.238	
B1e	-2.799	-0.160	0.051	-0.066	0.111	37	-0.091	0.147
B2	-1.947	-0.190		-0.184		258	-0.238	
B2e	-1.934	-0.148	0.042	-0.069	0.115	56	-0.169	0.069
B3-4	-1.381	-0.174		-0.162		236	-0.209	
B3-4e	-1.414	-0.152	0.022	-0.060	0.102	22	-0.153	0.056
B5-6	-0.916	-0.156		-0.144		386	-0.194	
B5-6e	-1.050	-0.157	-0.001	-0.060	0.084	19	-0.143	0.051
B7-8-9	-0.193	-0.132		-0.114		365	-0.153	
B7-8-9e	-0.490	-0.164	-0.032	-0.130	-0.016	2	-0.104	-0.049
A0	0.718	-0.062		-0.088		116	-0.124	
A0e	0.820	-0.155	0.093	-0.036	0.052	3	-0.076	0.048
A1-6	1.432	-0.011		-0.034		129	-0.103	
A1-6e	1.596	-0.014	0.003	-0.014	0.020	4	-0.165:	-0.062

¹ Averaged values of M_V , $(B - V)_0$ (Cols. 3, 8), $(V - I)_0$ (Col. 5), and difference in colour index between emission and non-emission line stars (Cols. 4 and 9 for $(B - V)_0$ and Col. 6 for $(V - I)_0$). Columns 8 and 9 provide data from [McSwain & Gies \(2005\)](#) stars in the Galaxy ("Galaxy"). Crude error estimates (1σ) are 0.054 mag for the SMC $(B - V)_0$ values, and 0.030 mag for the Galactic $(B - V)_0$ values.

However, the clusters studied are mainly young, among them NGC 6611. In this cluster, [Martayan et al. \(2008\)](#) have showed that some early-type objects remain on the pre-main-sequence. They also found that the rotational velocities of these two kinds of objects differ by about 20%, with ZAMS stars rotating more slowly. The theoretical models from [Meynet & Maeder \(2000\)](#) can explain this decrease with an internal redistribution of the angular momentum at the ZAMS.

If a difference between the rotational velocity of cluster and field stars is not caused by biased sampling of evolutionary effects but is related to local stellar density, the frequency of Be stars should be higher in open clusters than in the field at large, and also higher in higher-density fields. The WFI SMC database permits this comparison to be made. In a future paper, this hypothesis will be checked by dealing with SMC field stars. Accordingly, the star surface and space density of each open cluster in the sample was calculated and compared with the contents of its main-sequence emission-line stars (Oe, Be, Ae). No correlation between the two sets of quantities was evident (Fig. 9), in agreement with the findings of [McSwain & Gies \(2005\)](#) for Galactic clusters.

5.4. The Be phenomenon: SMC vs. Galaxy

In both galaxies, the fraction of near-main sequence Be stars varies significantly from one open cluster to the other. Although this finding is clearly established, it remains without a conclusive explanation. Not to be misled by these problems caused by small number statistics, all WFI SMC and all Galactic emission-line stars were combined to one sample each. The completeness of these samples with spectral type can be inferred from Fig. 10, which confirms that the SMC sample is incomplete towards fainter stars, i.e., later B subtypes, whereas in the Galaxy the increase toward later subtypes basically follows the initial mass function (IMF).

The global fractions of main-sequence Oe/Be/Ae stars per spectral subclass are provided in Table 4. As Fig. 11 illustrates, the distributions have similar overall shapes. However, with

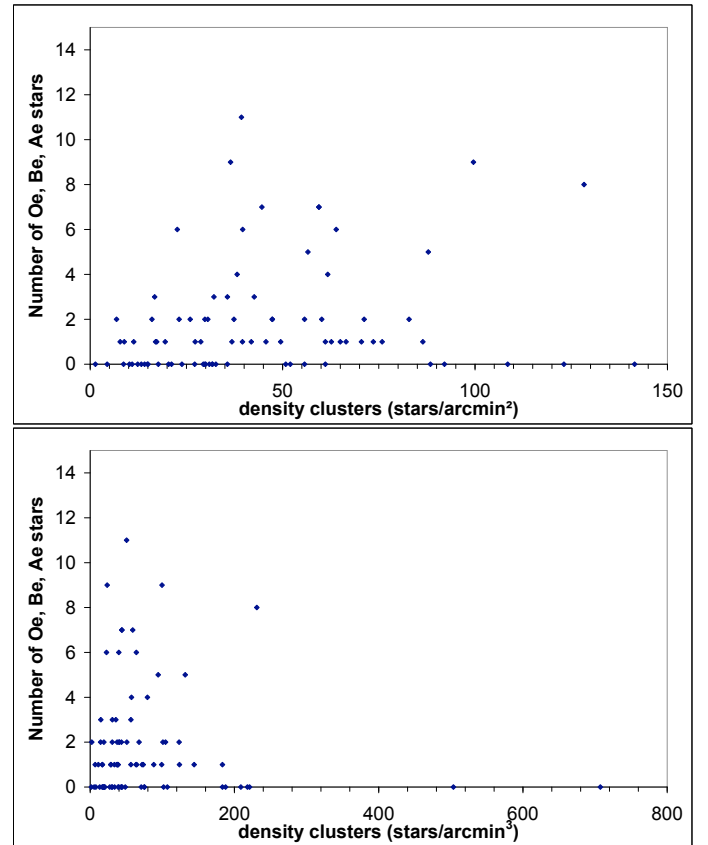


Fig. 9. Number of emission-line stars (Oe, Be, Ae) vs. area (*top*) or volume (*bottom*) density of SMC open clusters.

fractions reaching nearly 35%, early-type Be stars are more abundant in the SMC than in the Galaxy by a factor of 3–5. This factor drops to 2–4 if the very populous cluster NGC 330 is removed from the sample so that the overabundance of Be stars among early spectral subtypes is robust. The slitless study of

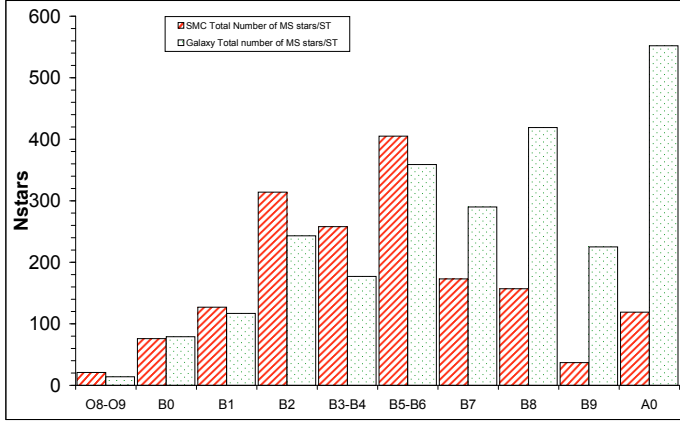


Fig. 10. Global fractions of main-sequence stars with and without emission lines as a function of spectral type (from O to early A stars). Left bars: SMC; right bars: Galaxy (from [McSwain & Gies 2005](#)). Both are similar and appear shaped by the initial mass function. However, in the SMC data the cut-off due to incompleteness sets in quite visibly at earlier spectral types (brighter magnitudes).

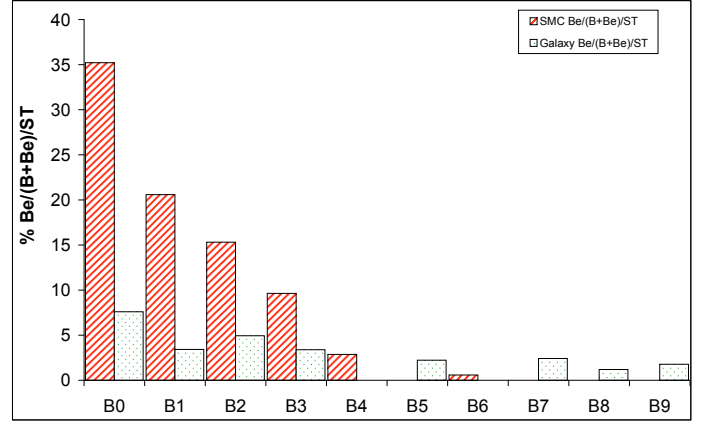


Fig. 11. The percentage of definite Be stars among all B-type (definite+candidate Be + B) stars vs. spectral type. Shaded bars: SMC; light bars: Galaxy.

Table 4. Number ratios of Be to (B+Be) stars as a function of spectral type in SMC and Galaxy¹.

Spectral type	SMC %	SMC % without NGC 330	Galaxy %
O8-O9e	23.8	20.8	14.3
B0e	35.2	26.3	7.6
all B0e	36.1		12.7
B1e	20.6	16.7	3.4
all B1e	27.0		7.7
B2e	15.3	13.9	4.9
all B2e	19.9		7.8
B3e	9.6	8.9	3.4
all B3e	14.0		6.8
B4e	2.9	3.0	0.0
all B4e	7.6		0.0
B5e	0.0	0.0	2.2
all B5e	1.8		9.2
B6e	0.6	0.6	0.0
all B6e	1.2		0.0
B7e	0.0	0.0	2.4
all B7e	0.0		7.2
B8e	0.0	0.0	1.2
all B8e	0.0		9.3
B9e	0.0	0.0	1.8
all B9e	0.0		11.1
A0e	2.5	2.5	0.9

¹ For each range in spectral type, the fractions of definite emission-line stars and the combination of definite and candidate emission-line stars are listed.

[Mathew et al. \(2008\)](#) reports similar Be-to-B star ratios in Galactic clusters as [McSwain & Gies \(2005\)](#) do.

We note that these three studies may be compared because they are all single-epoch studies. Since the Be phenomenon is transient, the true frequency of Be stars must be higher than apparent from these surveys. The study by [Fabregat \(2003\)](#) suggests that up to one-third of all Be stars may be missed at any one epoch. Studying the Galactic cluster NGC 3766, [McSwain et al. \(2008\)](#) even suggest that 25 to 50% of the Be stars could be missed in a single-epoch spectroscopic survey. This, of course, depends very much on the nature and quality of the data. We

note that it is not known whether the volatility of emission lines differs between the Galaxy and SMC. In the Galactic field, the variability of classical Be stars is significantly higher among the early spectral subtypes, to which the present study is limited.

The inclusion of candidate Be stars (Table 4) does not much affect the distribution function in the SMC. However, for the Galactic late-type candidate-Be stars from [McSwain & Gies \(2005\)](#) there is a large increase. It is conceivably due to the difficulty of distinguishing photometrically between either pre-main-sequence or Herbig Ae/Be stars and classical Be stars. The more frequent occurrence of these stars in young open clusters supports this interpretation.

5.5. The Be phenomenon as a function of spectral type

Figure 12 presents the percentages per spectral subclass, referred to the total sample of Be stars, but separately for SMC and Galaxy. The Galactic data are from [Zorec & Frémat \(2005\)](#), [McSwain & Gies \(2005\)](#), and [Mathew et al. \(2008\)](#). The distributions for the two galaxies are similar but the incompleteness of the SMC data becomes apparent beyond B2 (cf. Sect. 3.3) and prevents a more detailed comparison. The highest number of Be stars is encountered at spectral type B2 in both the SMC and Galaxy. Because this coincides with the maximum of the H α emission-line strength ([Zorec et al. 2007](#)) while for weaker line strengths the statistics are increasingly incomplete, it is questionable whether Fig. 12 displays the true dependency of the Be phenomenon on effective temperature. At late spectral subclasses, the more complete Galactic data level off to a plateau, as already shown by [Kogure & Hirata \(1982\)](#). As proposed by [Zorec & Frémat \(2005\)](#) and [Zorec et al. \(2007\)](#), this may be caused by the combination of the decreasing relative frequency of Be stars and the absolute increase in the number of late B stars with the initial mass function.

Unlike in Fig. 11, the distribution in Fig. 12 does not drop very quickly with spectral type because the total number of Be stars per spectral bin is roughly constant to within a factor of 2–3. This is not true in general for B-type stars because the IMF causes their numbers to increase rapidly towards lower temperatures.

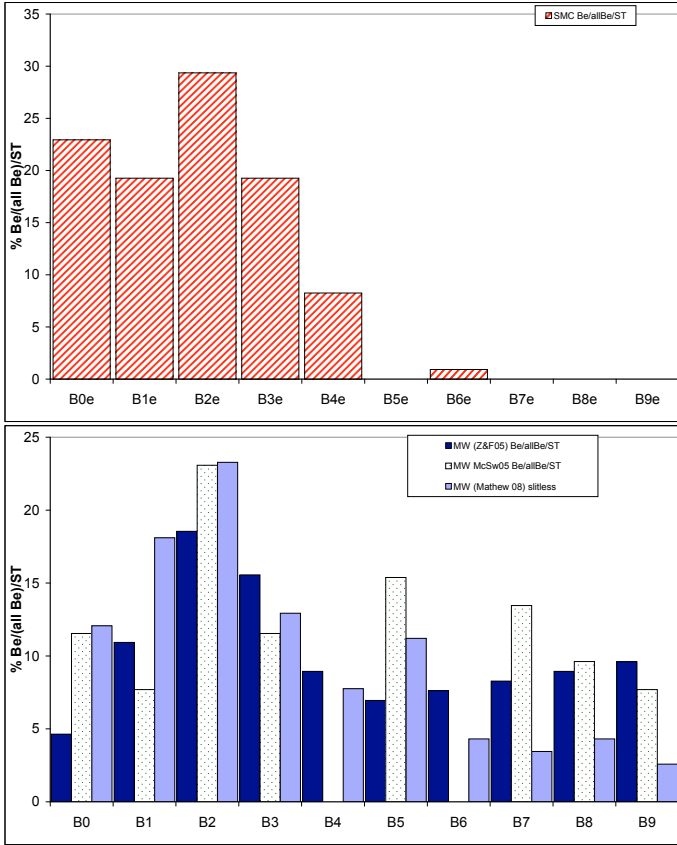


Fig. 12. The distribution of definite Be stars, as a percentage of the total number of Be stars in the sample, with spectral type in SMC (*top*, this paper, red dashed bars) and Galaxy (*bottom*). The data for the Galaxy are from Zorc & Frémat (2005, left blue bars), McSwain & Gies (2005, middle white bars), and Mathew et al. (2008, right, light blue bars).

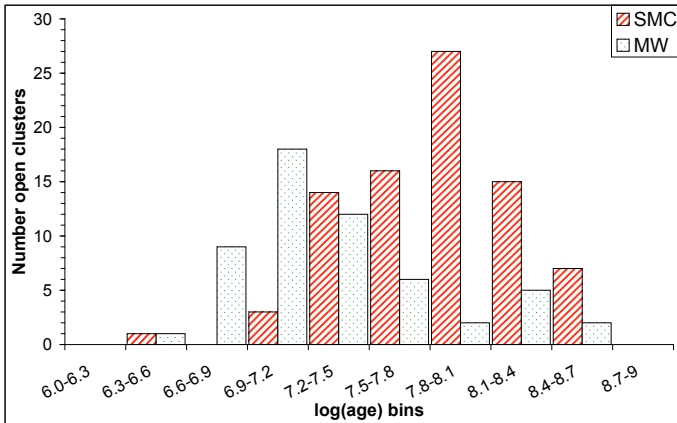


Fig. 13. The log(age) distributions of open clusters in SMC (left bars) and Galaxy (right bars, data from McSwain & Gies 2005).

5.6. Evolution and age

Figure 13 shows the distributions in age of the open clusters of the SMC (Pietrzynski & Udalski 1999) and Galactic samples. In the SMC sample, there are more old open clusters than in the Galactic one although the stellar population of the Galaxy is in general older than that of the SMC.

The number ratios of Be to B stars as a function of the age of open clusters in the SMC are shown in Fig. 14. For the Galaxy, we refer to Fig. 4 of McSwain & Gies (2005). There is a

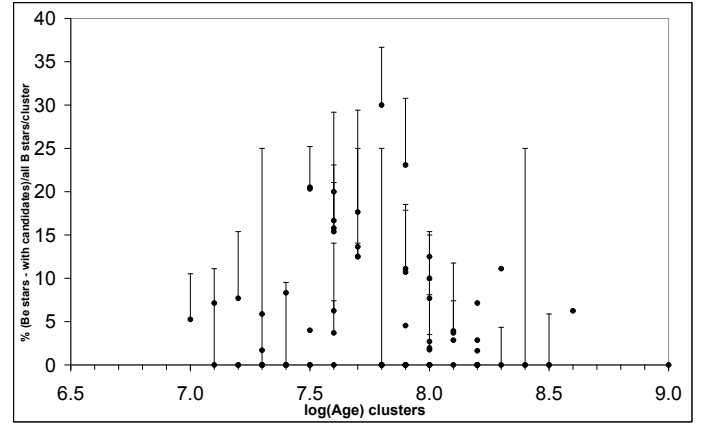


Fig. 14. Number ratio of Be to B stars vs. cluster age in the SMC. The circles correspond to definite Be stars only, and the vertical bars extend the values by the respective candidate Be stars. In comparison, Fig. 4 of (McSwain & Gies 2005), which is the equivalent diagram for Galactic clusters, is basically flat with cluster age.

maximum at log(age) ~ 7.6 in the SMC, while in the Galaxy no clear trend is seen. If taken at face value, there may represent a small evolutionary enhancement of Be stars in the SMC. However, a similar distribution may result already if the Be phenomenon peaks at a particular spectral sub-type.

Similarly, Fig. 15 presents the ratios of open clusters with Be stars to all open clusters by age bins as defined by Mathew et al. (2008, their Fig. 8); the top panel is for definite Be stars, and the bottom panel combines definite and candidate Be stars. The comparison is made with data in the Galaxy from Mathew et al. (2008) and McSwain & Gies (2005). As noticed in the Galaxy by Mathew et al. (2008), there seems to be a decrease first in the number of open clusters with Be stars towards 30–40 Myr (log(age) = 7.5–7.6). Thereafter, there is an increase during the evolution, and another decrease after 50–60 Myr (log(age) = 7.7–7.8). Figures 13 and 14 indicate that some Be stars could be born as Be stars (Wisniewski et al. 2007b), while others only happen to have Be characteristics during the evolution as mentioned by Fabregat & Torrejón (2000). The first decrease, if real (the differences between the studies being compared are large), could be caused by Be stars reaching the terminal-age main-sequence or by an evolutionary change in the angular velocities so that not every initial Be star can sustain a high enough surface rotation rate to remain a Be star throughout its entire main-sequence life (Martayan et al. 2007b).

Moreover, for both the Galaxy and at low metallicity, respectively, Meynet & Maeder (2000) and Maeder & Meynet (2001) showed that, while the linear rotational velocity decreases with time, the fractional critical angular velocity (Ω/Ω_c) increases. This holds for both medium- and low-mass B-type stars over the range of metallicity studied and for massive B-O stars of low metallicity. However, in massive Galactic-metallicity stars, Ω/Ω_c decreases with age because of the larger losses in mass and angular momentum.

From observations of Galactic Be stars with $\Omega/\Omega_c \geq 70\%$, Martayan et al. (2007b, Fig. 11) reckon that massive Be stars lose their emission-line characteristics after a few million years, while late-type Be stars begin to appear at 40% of their main-sequence lifetime or nearly 40 million years. This is the age, at which (Fig. 15) the fraction of open clusters with Be stars begins to rise again. For an SMC-like metallicity, Martayan et al. (2007b, Fig. 11) predict that massive and intermediate-mass Be

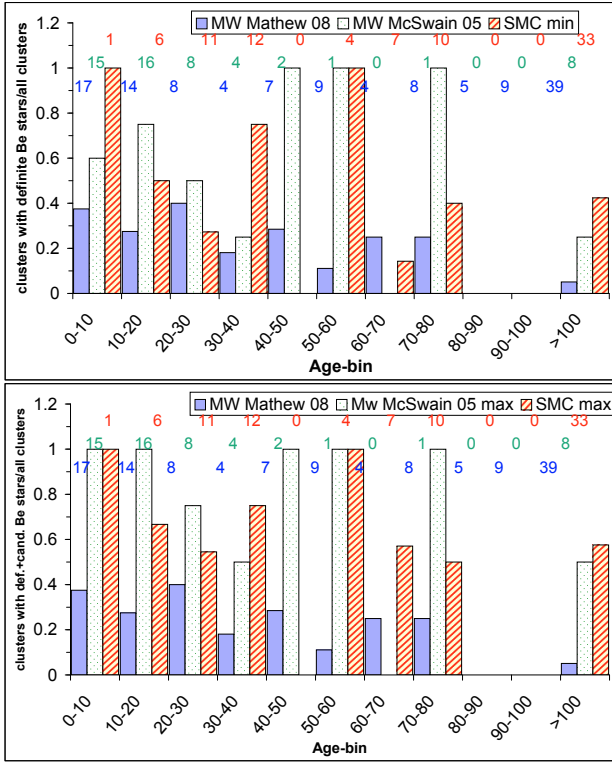


Fig. 15. Fraction per age bin of open clusters with Be stars in the Galaxy and SMC (following Fig. 8 of Mathew et al. 2008); *top*: definite Be stars, *bottom*: definite+candidate Be stars. The data for the Galaxy are from Mathew et al. (2008, left blue bars), McSwain & Gies (2005, middle white bars), and for the SMC (this study, right red bars). Numbers at the top show the absolute numbers represented by each bar.

stars appear between 3 and 5 million years. At intermediate cluster ages, the fraction of clusters hosting Be stars decreases because this massive population disappears when it reaches the TAMS. Finally, at an age of about 35–45 million years and an SMC metallicity, late-type Be stars began to form. This expectation, based on the evolution of Ω/Ω_c as a function of metallicity and mass, is qualitatively matches the distribution in Fig. 15.

To investigate age dependencies further, Fig. 16 presents the range in $\log(\text{age})$ of the host clusters as a function of spectral type (data from McSwain & Gies (2005); recall that the Be stars in the SMC were “selected as main-sequence stars”). In the Galaxy, early-type Be stars are found close to the terminal-age main-sequence stars, intermediate-mass Be stars are mainly evolved, and definite late-Be stars are also evolved. The late-type candidate Be stars could be unevolved but there is a potential risk of confusion with pre-main sequence objects. The Be stars seem to follow the evolutionary scheme described in Fabregat & Torrejón (2000), Zorec et al. (2005), and Martayan et al. (2007b), depending on their mass.

In the SMC, the OGLE ages (Pietrzynski & Udalski 1999) of some clusters do not closely agree with their having very early-type stars (O-B0) as members. One example is Ogle-SMC72 with $\log(\text{age}) = 7.6 \pm 0.2$ which contains 3 B0e stars, although B0 stars reach the terminal-age main-sequence already at $\log(t) = 7$.

On the other hand, Chiosi et al. (2006) derived $\log(\text{age}) = 6.6 \pm 0.5$ for this cluster, which is fully consistent with B0e member stars. There are also differences between the ages from Pietrzynski & Udalski (1999) and Chiosi et al. (2006) for other open clusters in the WFI sample, which could

explain some of the discrepancies between individual spectral types and parent-cluster ages. Even though in some specific clusters the ages published by Chiosi et al. (2006) are in better agreement with the presence of Be stars, this is not generally the case.

If all OGLE ages from Pietrzynski & Udalski (1999) are taken at face value, 55% of the Be stars, which were selected as main-sequence stars, could be younger than their host clusters. With the ages from Chiosi et al. (2006), this value reaches 62%. As the published error estimates are lower for Pietrzynski & Udalski (1999), their estimates were adopted. If the problem is not due to either the assigned ages or the TAMS calibration, all possible explanations for blue stragglers (e.g., multi-epoch or continuous star formation, mass-transfer binaries, etc.) are potential candidates. This hypothesis could be reinforced by the finding that Be/X-ray binaries are more abundant in the SMC than in the Galaxy according to Haberl & Sasaki (2000), who explain this result with different star-formation histories of the two galaxies.

On the other hand, the colour–magnitude diagrams in Sect. D and the location of blue stragglers as delineated by Ahumada & Lapasset (2007) suggest that at most a few Be stars are in the blue-straggler zone while most Be stars are on the red side of the cluster main sequences. As discussed in Sect. 5.2, this is probably unrelated to their age.

The other main-sequence Be stars, located below the TAMS, are found evolved to the second part of the main-sequence, in agreement with the evolutionary picture sketched by Fabregat (2003) and Martayan et al. (2007b) for intermediate-mass Be stars in the SMC. The emission-line stars in NGC 346 could be either classical Be stars or pre-main-sequence stars such as Herbig Ae/Be stars. This would mostly affect the late spectral subtypes but at B0 some pre-main-sequence stars are also found (Nota et al. 2006).

Both in the SMC and Galaxy, diagrams such as Fig. 16 but for non-emission-line B stars show a uniform distribution with the age of the open clusters.

In the SMC, Be stars are mostly located in the region corresponding to the second half of the main-sequence (except for some late-type stars in NGC 346, but they could well be pre-main-sequence stars), in agreement with the results of Fabregat & Torrejón (2000) and Martayan et al. (2007b). However, the lack of open clusters with ages corresponding to the first half of the main-sequence evolution of B-type stars makes it impossible to conclude that the Be phenomenon is *restricted* to the second half of the main-sequence evolution.

In the Galaxy, definite Be stars (red circles in Fig. 16, bottom panel) have mostly evolved to the second half of the main-sequence band as reported before by Fabregat & Torrejón (2000). The earliest (B0e) have already reached the TAMS. The locations of candidate and definite Be stars with early spectral types largely overlap. Towards later spectral sub-types, candidate Be stars may be either less or even unevolved. However, there is a risk of confusion with pre-main sequence objects. This uncertainty is smaller for definite Be stars.

To confirm the nature and to determine the evolutionary status of these Be stars reliably, spectra of both higher resolution and wider spectral coverage are required for both young and medium-aged open clusters in the SMC as well as in the Galaxy.

A new result suggested by the present study is that in the SMC the Be phenomenon is more enhanced towards hotter and more massive stars (O stars) than in the Galaxy. Because the losses of mass and angular momentum are lower in the SMC than in the Galaxy, this result is plausible and qualitatively

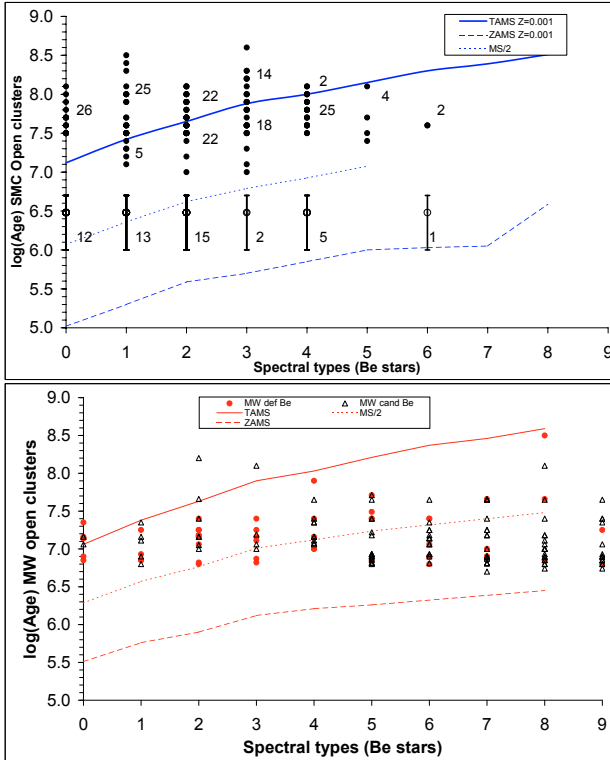


Fig. 16. Spectral types of Be stars vs. log (age) of their host clusters in SMC (*top*) and Galaxy (*bottom*). The curves show terminal- and zero-age main sequence and the main-sequence half-age following Schaller et al. (1992), with $Z = 0.001$ for SMC and $Z = 0.020$ for the Galaxy). In the SMC, the numbers are the absolute numbers of stars in each spectral subtype, and the open circles with large age error bars correspond to the emission-line stars in NGC 346. In the Galaxy, the circles denote the definite Be stars and the triangles identify the candidate Be stars.

consistent with the theoretical prediction of Maeder & Meynet (2001). However, these authors did not quantify the expected fractions of Oe or Be stars as a function of metallicity.

An important parameter to consider is Ω/Ω_c , the fractional critical angular rotation rate. If low-metallicity stars form with about the same initial angular momentum as more metal-rich stars of equal mass but have smaller radii on the main sequence, their Ω/Ω_c values must be higher.

Since the, expected higher relative frequency of Be stars is higher in the SMC than in the Galaxy, Ω/Ω_c may be the parameter that controls the formation of rapidly rotating B stars. They may become Be stars because of their rapid rotation. Alternatively, the Be phenomenon may be assisted by pulsation-assisted outbursts, which are triggered by the beating of two or more non-radial pulsations modes. In the Galaxy, only one such case has been found so far (μ Cen, Rivinius et al. 1998). However, several photometrically multi-periodic candidates were identified by Martayan et al. (2007a) and Diago et al. (2008) in the SMC. The latter authors report an order of magnitude higher incidence of pulsations among Be stars than in B stars without emission lines.

In summary, the results of this work indicate that, at least for single stars, the Be phenomenon is coupled to (initial) mass, evolutionary stage, and metallicity. However, it is not evident that these 3 parameters are primary quantities determining the prevalence of the Be phenomenon. A more physical description, in accordance with the above, is that by Martayan et al. (2007b), who propose that the Be phenomenon depends primarily on the

evolution of Ω/Ω_c . the ratio Ω/Ω_c is also governed by evolutionary stage and metallicity but the dependencies are different between different mass domains, causing to the confusing apparent lack of consistency or uniqueness of empirical studies of the Be phenomenon in general (the larger the area “imaged”, the more single trees seem to stand out).

6. Summary and conclusions

A slitless spectroscopic survey for emission-line objects in the SMC was performed, which contained 14 fields covering most of the SMC. From 3 million spectra, about 8120 spectra of 4437 stars in 84 clusters and 14 nearby comparison fields were automatically selected. The final database comprises 122 definite main-sequence Oe/Be/Ae stars and 54 candidate emission-line stars, 1659 main-sequence O/B/A stars, 2408 other normal stars, and 90 emission-line stars that are not close to the main sequence. Fifty-five emission-line stars in NGC 346 were also found and classified; but their nature – either main-sequence or pre-main-sequence stars – is not clear, so they were not included in the statistics and analysis.

Cross-correlation with the OGLE database permitted these emission-line objects to be associated with homogeneous photometric data. For 49 additional emission-line stars, photometric data could not be derived. While the survey is spatially homogeneous, it starts to become incomplete around B3 (on the main sequence). For comparison, similar Galactic (but photometric) data from the work of McSwain & Gies (2005) were converted to the same scales in absolute luminosity and effective temperature.

Careful analysis led to the following conclusions:

- An intercomparison of clusters did not show any dependency of the relative frequency of emission-line stars on spatial density.
- In the SMC, the Be phenomenon is more strongly enhanced towards early-type stars (O stars) than in the Galaxy. Among early spectral subtypes, the fraction of Be stars in the SMC exceeds that in the Galaxy by a factor of ~ 3 –5.
- The largest number of Be stars is found at spectral type B2 in both the SMC and Galaxy. Since the emission-line strength also is at its largest near B2, this result is difficult to reconcile with the presence of low sensitivity to weak emission lines.
- In color-magnitude diagrams, most Be stars are found off the zero-age main-sequence, with many of them defining a separate red “sequence”.
- The age distribution of clusters hosting Be stars shows that the Be phenomenon covers the second half of the main-sequence evolution. Some Be stars may have formed as Be stars, while others may have acquired their Be nature only during the course of their evolution. There are not enough young clusters in the SMC sample to say anything about the Be phenomenon during the first half of the main-sequence evolution of SMC stars.
- The observations are consistent with Ω/Ω_c being one of the main quantities governing the statistics of emission-line stars in all subsamples of single stars. The ratio Ω/Ω_c rises slowly with time for intermediate and late B stars of all metallicities, for massive B and O stars. The same holds for early-type B stars with SMC metallicity. Only massive Galactic OB stars are different in that their Ω/Ω_c decreases with time. When also evolution, initial mass, and metallicity are considered, the relative abundance of Be stars takes on a multi-parametric appearance although Ω/Ω_c continues to dominate.

The above trends only stand out significantly in sufficiently large samples. Seemingly very similar, if not identical, small samples (e.g., single open star clusters) can differ drastically in their number of Be stars. To date, there is not even a speculative explanation for this. Maybe, a large variation in the initial distribution of rotation rates combined with a threshold in Ω/Ω_c plays a role.

In forthcoming articles, we shall present results of WFI slitless H α spectroscopy in the SMC field (outside clusters), and in both open clusters and the field of the LMC. The nature of emission-line stars far from the main sequence will also be studied further in a future paper.

Acknowledgements. The authors acknowledge the referee for valuable comments that helped to present the essence of the paper more clearly. C.M. thanks Drs. A.-M. Hubert, M. Floquet, and Y. Frémat for sharing useful information during the preliminary analysis of our data. Dr. E. Bertin's adaptation of his *SExtractor* package proved most helpful for the mass reduction of the observations. This research has made use of the Simbad and VizieR databases maintained at CDS, Strasbourg, France, of NASA's Astrophysics Data System Bibliographic Services, and of the NASA/IPAC Infrared Science Archive, which is operated by the Jet Propulsion Laboratory, California Institute of Technology, under contract with the U.S. National Aeronautics and Space Administration. This publication makes use of data products from the Two Micron All Sky Survey, which is a joint project of the University of Massachusetts and the Infrared Processing and Analysis Center/California Institute of Technology, funded by the U.S. National Aeronautics and Space Administration and the U.S. National Science Foundation. C.M. is grateful for support from ESO's DGDF in 2006.

Appendix A: Comments on individual open clusters

A.1. NGC 330 (Ogle-SMC107)

NGC 330 is a well-studied open cluster known for its high content of Be stars (see for example Keller et al. 1999). The area covered by NGC 330 is the largest one of all clusters in this paper. A total of 400 spectra was examined and 55 emission-line stars were identified. By cross-matching with OGLE photometry, we found that the majority of the emission-line stars are actually Be stars.

A.2. Bruck 60 (Ogle-SMC72)

Bruck 60 is one of the six SMC open clusters observed by Wisniewski & Bjorkman (2006). They found 26 Be stars, among them 6 Be-star candidates, within a radius of 1.5', while the present study extends over a radius of 35'' centered on the cluster. The two areas have 17 stars in common, of which *Album* rejected 8 highly blended sources. The detection rate of 9/17 stars is consistent with the estimated general extraction efficiency of 60% in the region of Bruck 60. Of the 9 detected stars (WBB_e5, WBB_e6, WBB_e7, WBB_e10, WBB_e17, WBB_e20, WBB_e21, WBB_e23, WBB_e25), 2 (WBB_e23 and WBB_e25) are not properly separated and were also eliminated. Of the 7 remaining emission-line stars, 4 (WBB_e5, WBB_e10, WBB_e17, WBB_e20) are in common to both studies. One star (WBB_e7), for which Wisniewski et al. (2007b) did not publish polarimetry, is found not to have emission. The two others (WBB_e6 and WBB_e21) are faint and have a too low S/N to provide a reliable conclusion about the presence of emission in their spectra. The stars poorly separated and/or with low S/N have *V* magnitudes of 17.4, 17.6, 18, and 18. Finally, the present study finds one candidate emission-line star not identified by Wisniewski & Bjorkman (2006).

A.3. NGC 346

This open cluster is highly complex with various subaggregates. Bouret et al. (2003) published an age of 3 Myr and a metallicity

of 0.004. However, Nota et al. (2006) found several populations with different ages: 4.5 Gyr for stars in the field, a young population with ages ranging from 3 to 5 Myr, in which stars with a mass less than 3 M_{\odot} are still pre-main sequence stars, and a population with an intermediate age of 150 Myr.

In this open cluster and in its vicinity, we found 55 emission-line stars. Dereddening with a global value of 0.008 mag for massive stars from Hennekemper et al. (2008) suggests that most of them are on the main sequence. The spectral classification obtained differs on average by 1 spectral subtype for the 12 stars shared with spectral classifications by other authors.

Table A.1 provides basic parameters for the 55 emission-line stars in NGC 346 along with magnitudes from the EIS pre-flames survey (Momany et al. 2001), from DENIS (Epchtein et al. 1994), and from 2MASS (Skrutskie et al. 2006). In Table A.2, other parameters are given as well as spectral classifications from WFI and other sources. Owing to the large spread in age of the stars in this cluster, some of them could be pre-main-sequence stars. Where possible, cross-references to the studies by Hennekemper et al. (2008), Wisniewski & Bjorkman (2006), Wisniewski et al. (2007b), and Hunter et al. (2008) and to the Simbad database are, therefore, also included.

Since the distinction between pre-main sequence (Herbig Ae/Be or T Tauri stars), main-sequence (mostly classical Be stars), and post-main-sequence emission-line stars (e.g., WR) requires more spectroscopic data of higher spectral resolution and wider area coverage, and also more complete membership in the different subclusters, the stars from NGC 346 were not included in the overall analyses of this paper. Their large number may have introduced biases.

Figure A.1 shows part of a WFI image with NGC 346. Most of the emission-line stars are identified. For the central parts of the cluster(s), Hennekemper et al. (2008) report numerous pre-main-sequence T Tauri stars, which are unfortunately too faint (see Fig. 4) to be detected by the present study. Figure A.1 also illustrates the ability of the WFI slitless spectroscopy to distinguish true circumstellar line emission from diffuse nebular emission. In low-resolution short-slit spectra, the difference can be marginal.

Appendix B: Open clusters: tables

Table B.1 lists all open SMC clusters with their basic properties as well as the WFI field(s) covering it. Also shown are the numbers and types of emission-line stars found in each WFI image. The results after merger of multiple observations are contained in Table B.2.

Appendix C: Tables of Oe/Be/Ae stars, and other emission-line stars

The following tables include information (e.g. astrometry, apparent and dereddened photometry, classification) for each emission-line star found.

Appendix D: HR diagrammes for individual open clusters

Colour/magnitude (M_v , $(B - V)_0$) diagrams are presented separately for each open cluster in the SMC with at least 10 members and at least 1 WFI emission-line star with OGLE photometry Udalski et al. (1998).

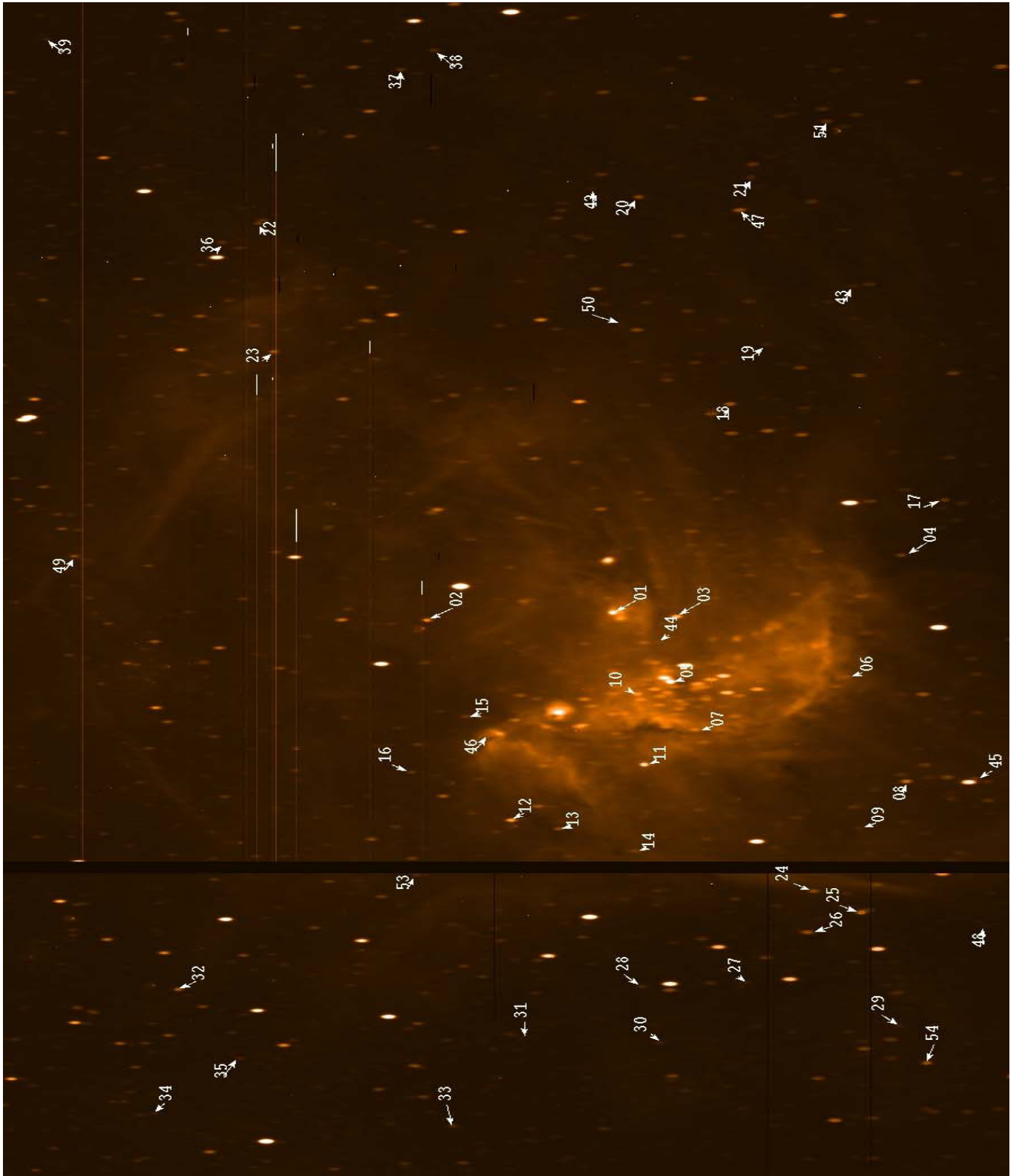


Fig. A.1. Part of a WFI spectral image showing NGC 346 and its vicinity. The sources appear elongated due their spectral nature. North is at the top, west to the right. The broad black vertical line is due to a gap between CCDs in the WFI mosaic. Arrows with numbers identify most of the emission-line stars, which can be found in Table A.1. This figure shows that the slitless spectroscopy allows to find circumstellar (CS) emission-line stars while slit-spectroscopy cannot disentangle CS and nebular emission lines in diffuse emission nebulae. According to [Hennekemper et al. \(2008\)](#), there are many pre main sequence T Tauri stars in the central regions of the cluster. But they are too faint to be detected here.

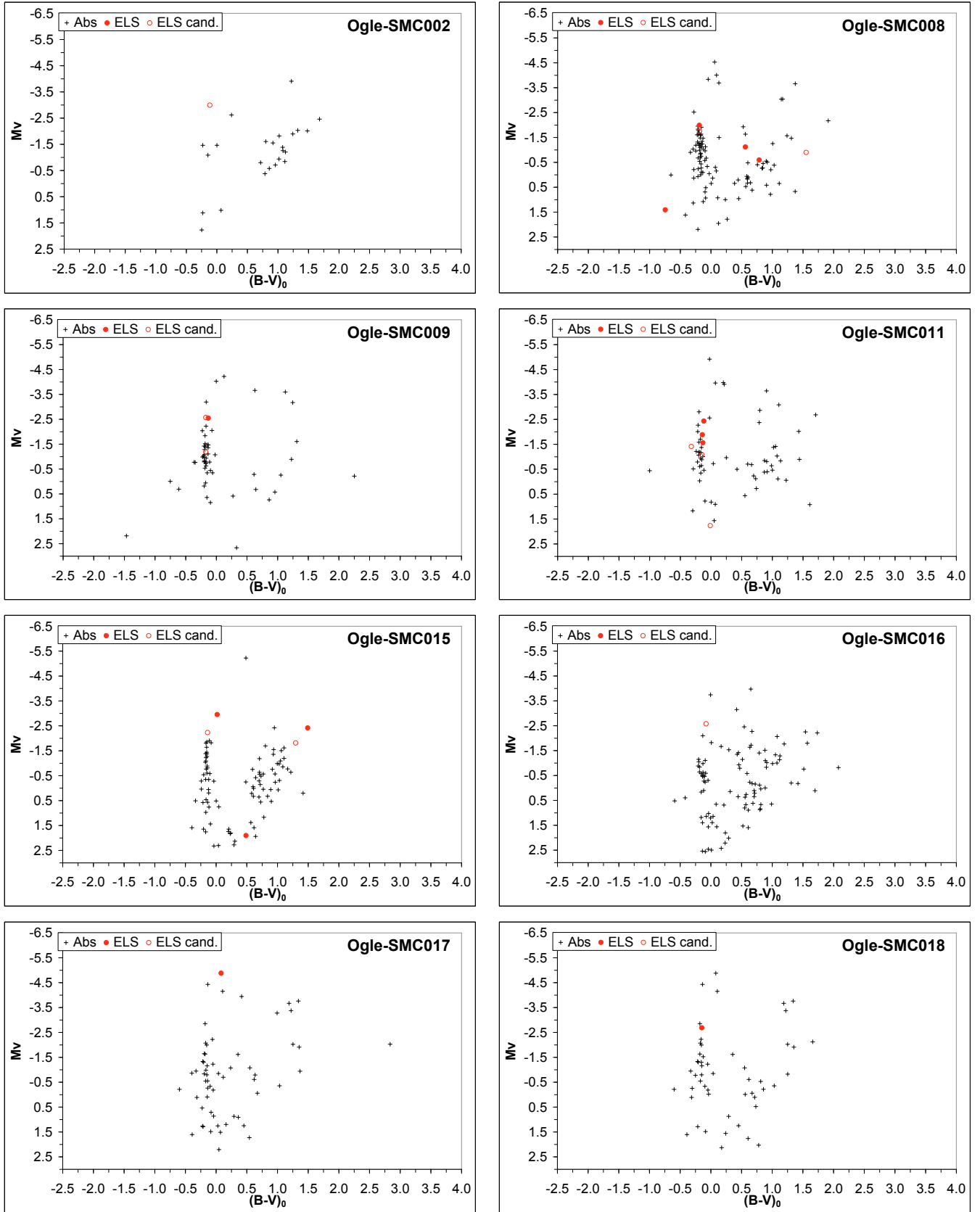


Fig. D.1. Dereddened colour $(B - V)_0$, absolute magnitude M_V diagrams for open clusters in the SMC with at least 10 stars and at least 1 emission-line star (red filled circle) or candidate emission-line star (red opened circle). Normal stars appear as black “+”. The identification of each open cluster is given in the top right corner.

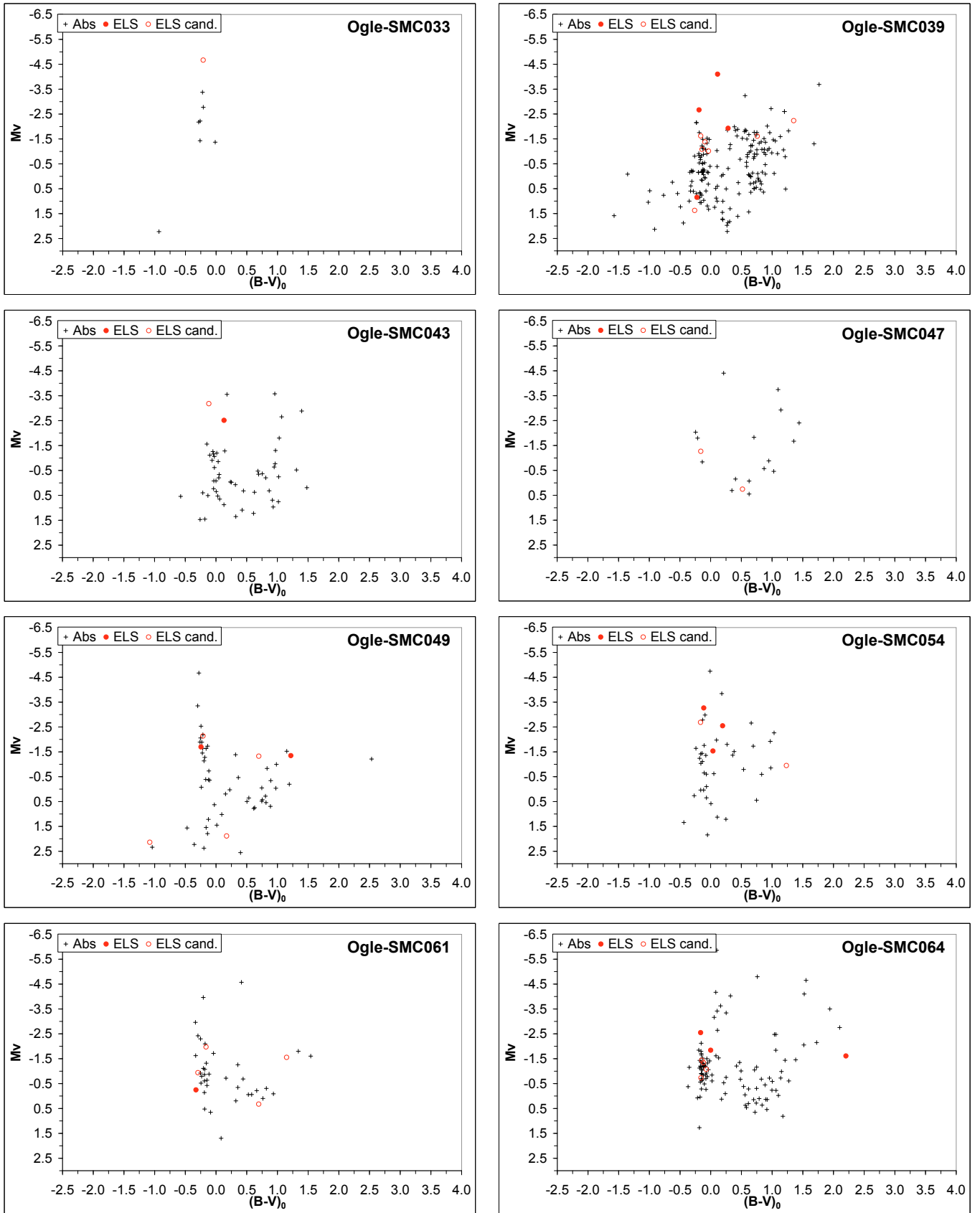


Fig. D.2. Same caption as for Fig. D.1.

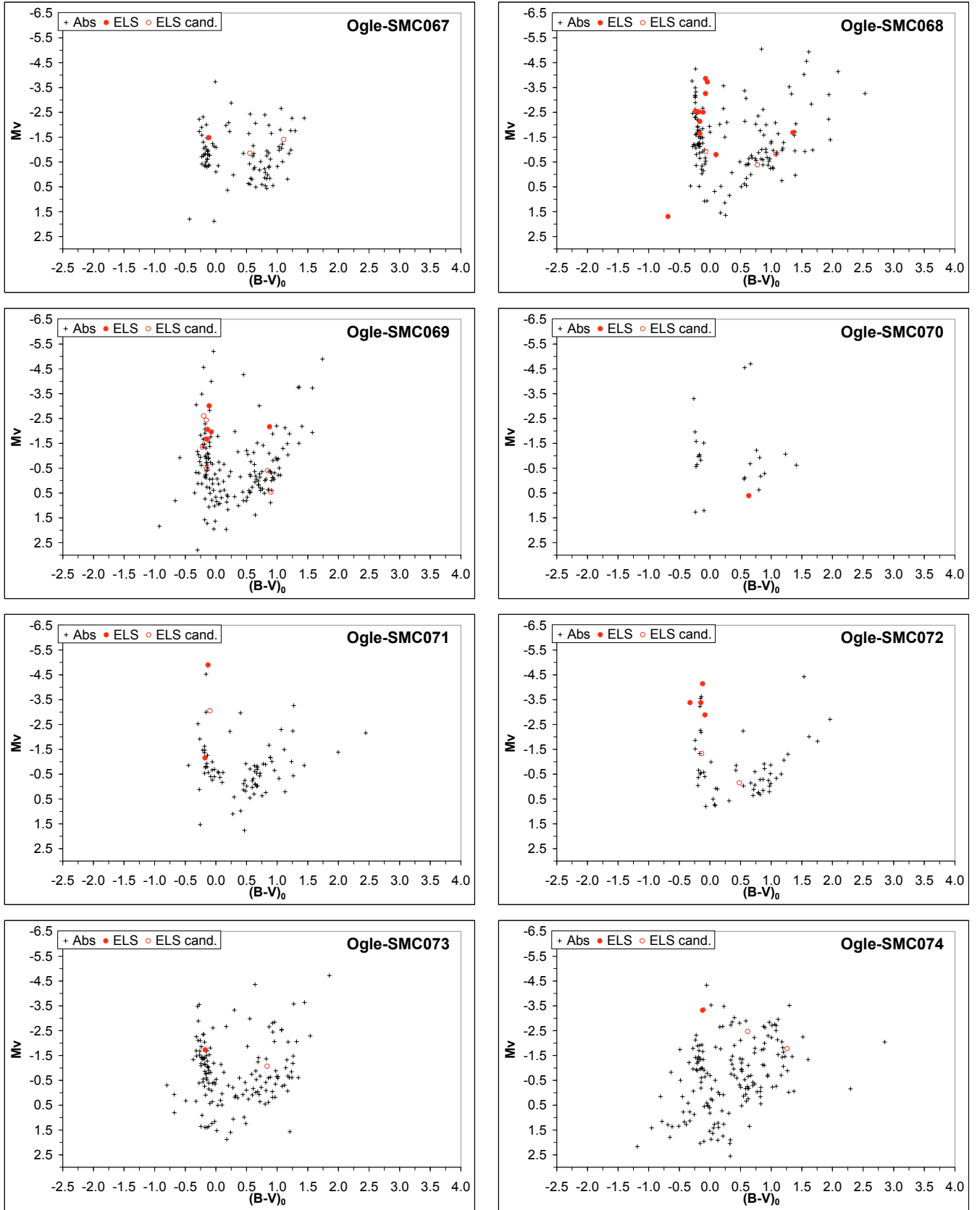


Fig. D.3. Same caption as for Fig. D.1.

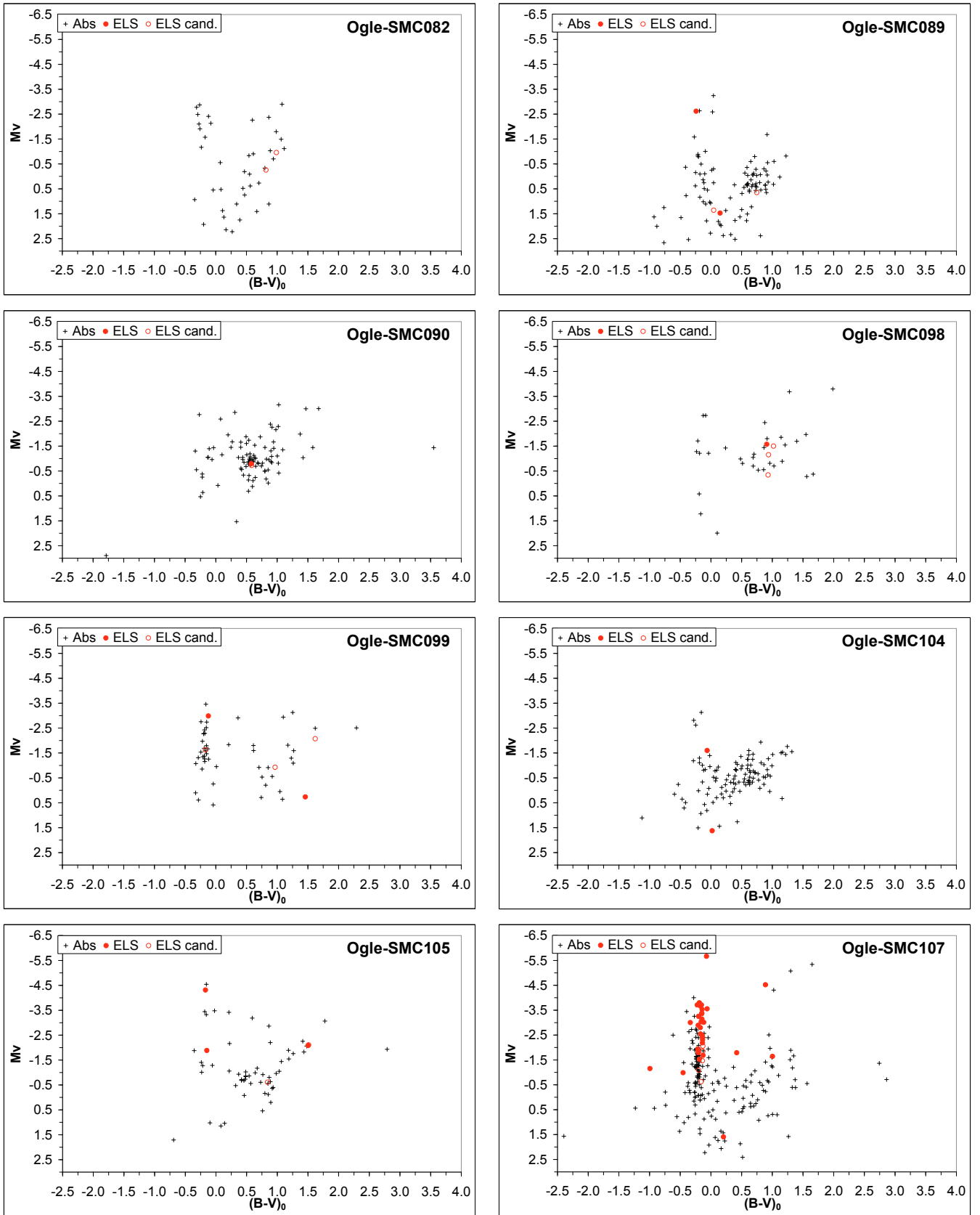


Fig. D.4. Same caption as for Fig. D.1.

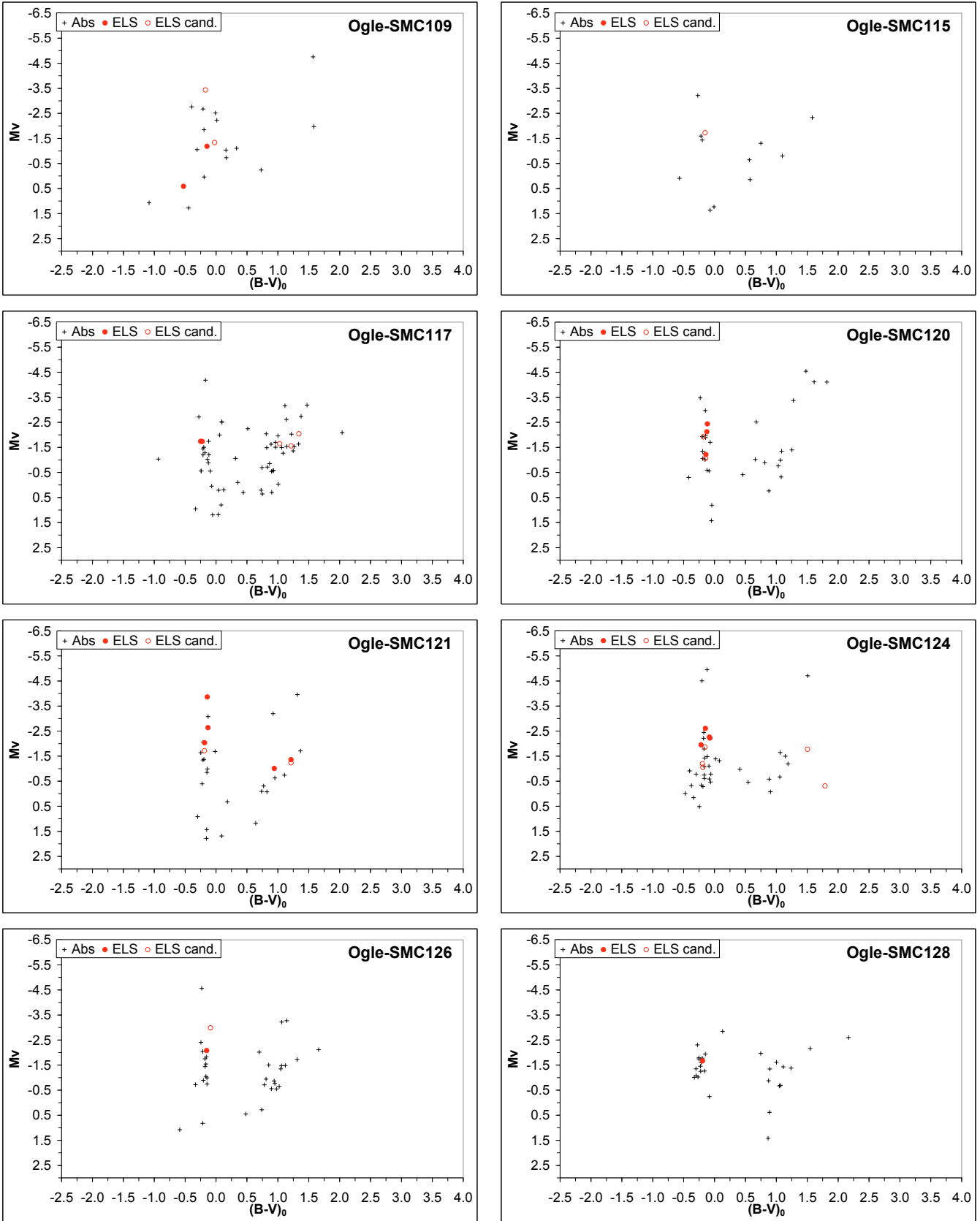


Fig. D.5. Same caption as for Fig. D.1.

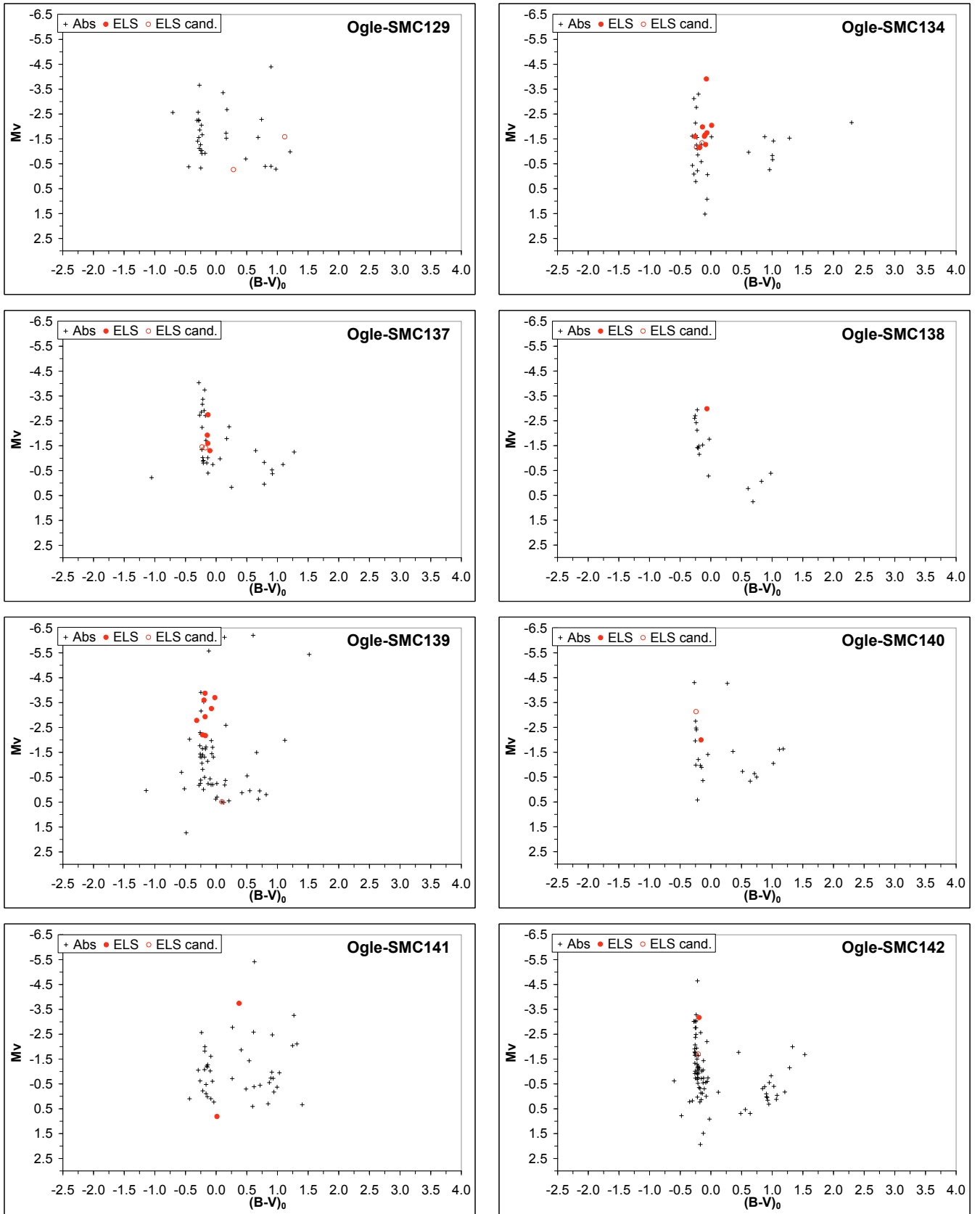


Fig. D.6. Same caption as for Fig. D.1.

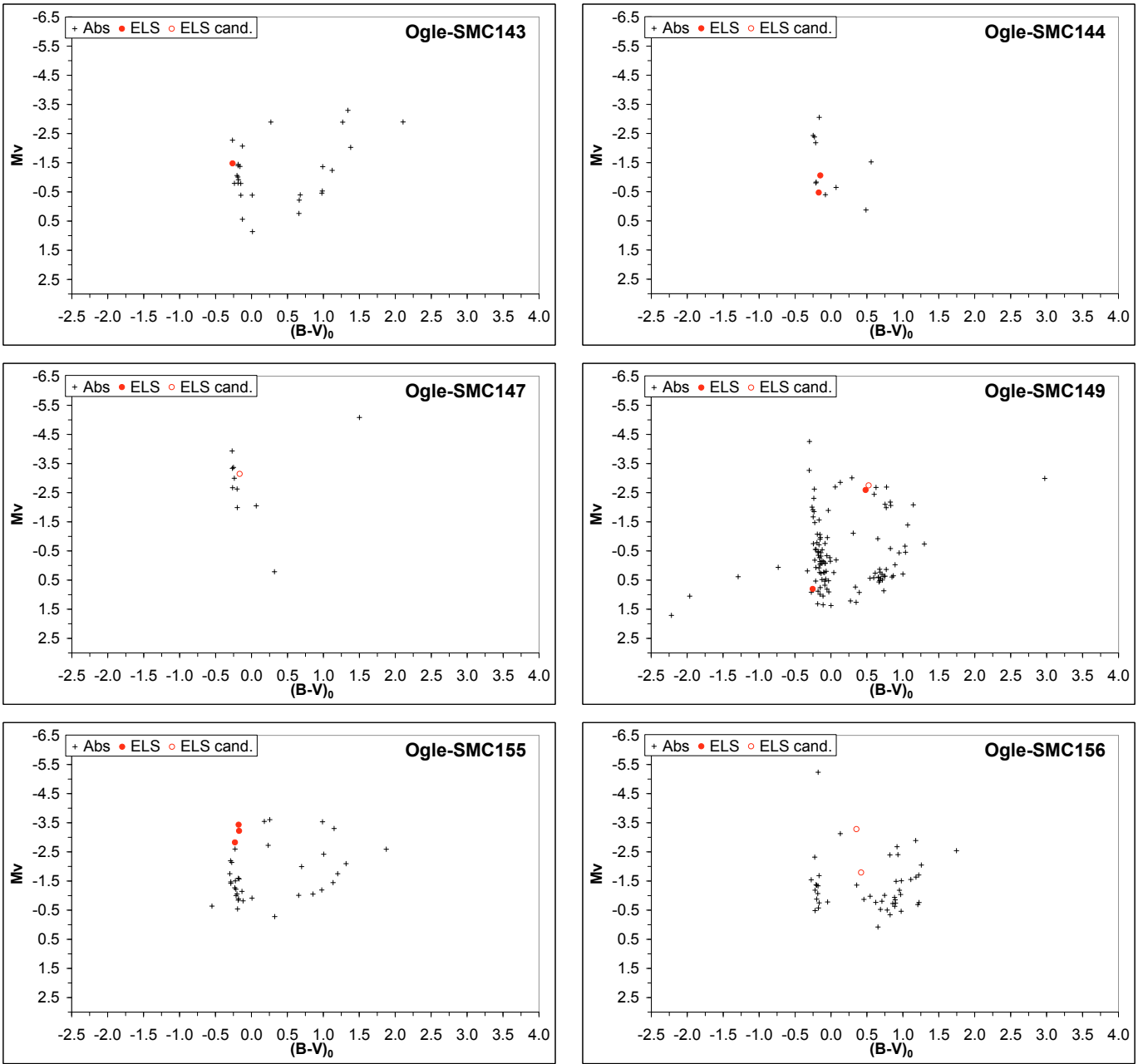


Fig. D.7. Same caption as for Fig. D.1.

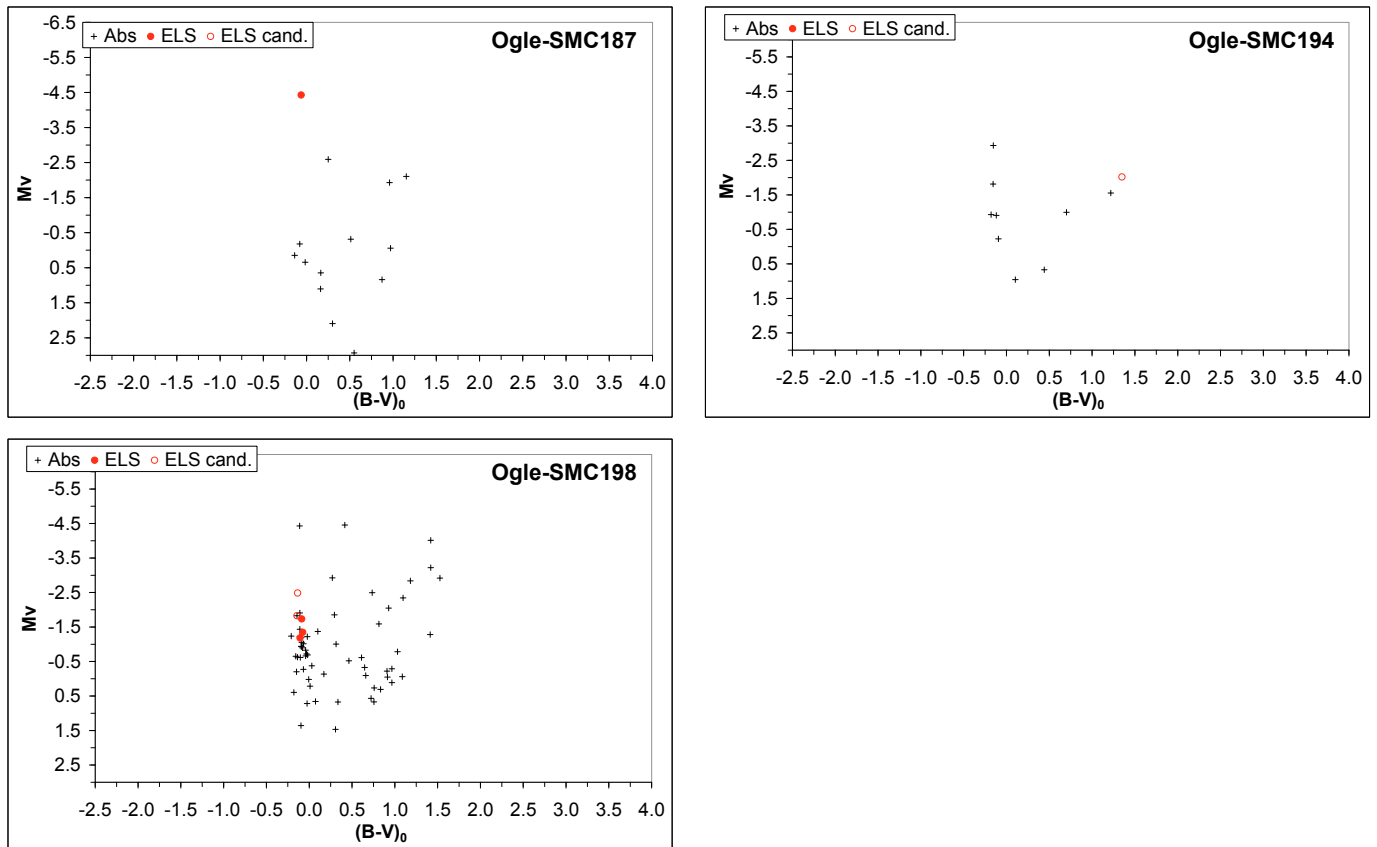


Fig. D.8. Same caption as for Fig. D.1.

References

- Ahumada, J. A., & Lapasset, E. 2007, *A&A*, 463, 789
- Baade, D., Meisenheimer, K., Iwert, O., et al. 1999, *The Messenger*, 95, 15
- Bertin, E., & Arnouts, S. 1996, *A&AS*, 117, 393
- Chiosi, E., Vallenari, A., Held, E. V., Rizzi, L., & Moretti, A. 2006, *A&A*, 452, 179
- Cioni, M.-R. L., Girardi, L., Marigo, P., & Habing, H. J. 2006, *A&A*, 452, 195
- Cousins, A. W. J. 1987, *South African Astronomical Observatory Circular*, 11, 93
- Cousins, A. W. J., & Caldwell, J. A. R. 1985, *The Observatory*, 105, 134
- Dachs, J., Kiehling, R., & Engels, D. 1988, *A&A*, 194, 167
- Diago, P. D., Gutiérrez-Soto, J., Fabregat, J., & Martayan, C. 2008, *A&A*, 480, 179
- Epchtein, N., de Batz, B., Copet, E., et al. 1994, *Ap&SS*, 217, 3
- Evans, C., Hunter, I., Smartt, S., et al. 2008, *The Messenger*, 131, 25
- Fabregat, J. 2003, in *Interplay of Periodic, Cyclic and Stochastic Variability in Selected Areas of the H-R Diagram*, ed. C. Sterken, ASP Conf. Ser., 292, 65
- Fabregat, J., & Torrejón, J. M. 2000, *A&A*, 357, 451
- Frémat, Y., Zorec, J., Hubert, A.-M., & Floquet, M. 2005, *A&A*, 440, 305
- Haberl, F., & Sasaki, M. 2000, *A&A*, 359, 573
- Hennekemper, E., Gouliermis, D. A., Henning, T., Brandner, W., & Dolphin, A. E. 2008, *ApJ*, 672, 914
- Huang, W., & Gies, D. R. 2006, *ApJ*, 648, 580
- Hummel, W., Szeifert, T., Gässler, W., et al. 1999, *A&A*, 352, L31
- Hummel, W., Gässler, W., Muschiolok, B., et al. 2001, *A&A*, 371, 932
- Hunter, I., Lennon, D. J., Dufton, P. L., et al. 2008, *A&A*, 479, 541
- Keller, S. C. 2004, *PASA*, 21, 310
- Keller, S. C., Wood, P. R., & Bessell, M. S. 1999, *A&AS*, 134, 489
- Kogure, T., & Hirata, R. 1982, *Bulletin of the Astronomical Society of India*, 10, 281
- Lang, K. R. 1992, *Astrophysical data, Planets and Stars* (New York: Springer Verlag)
- Maeder, A., & Meynet, G. 2001, *A&A*, 373, 555
- Maeder, A., Grebel, E. K., & Mermilliod, J.-C. 1999, *A&A*, 346, 459
- Martayan, C., Frémat, Y., Hubert, A.-M., et al. 2006, *A&A*, 452, 273
- Martayan, C., Floquet, M., Hubert, A. M., et al. 2007a, *A&A*, 472, 577
- Martayan, C., Frémat, Y., Hubert, A.-M., et al. 2007b, *A&A*, 462, 683
- Martayan, C., Floquet, M., Hubert, A. M., et al. 2008, *A&A*, 489, 459
- Mathew, B., Subramaniam, A., & Bhatt, B. C. 2008, *MNRAS*, 388, 1879
- McSwain, M. V., & Gies, D. R. 2005, *ApJS*, 161, 118
- McSwain, M. V., Huang, W., Gies, D. R., Grundstrom, E. D., & Townsend, R. H. D. 2008, *ApJ*, 672, 590
- Meynet, G., & Maeder, A. 2000, *A&A*, 361, 101
- Meyssonner, N., & Azzopardi, M. 1993, *A&AS*, 102, 451
- Momany, Y., Vandame, B., Zaggia, S., et al. 2001, *A&A*, 379, 436
- Nota, A., Sirianni, M., Sabbi, E., et al. 2006, *ApJ*, 640, L29
- Pietrzynski, G., & Udalski, A. 1999, *Acta Astron.*, 49, 157
- Porter, J. M., & Rivinius, T. 2003, *PASP*, 115, 1153
- Rivinius, T., Baade, D., Stefl, S., et al. 1998, *A&A*, 336, 177
- Schaller, G., Schaerer, D., Meynet, G., & Maeder, A. 1992, *A&AS*, 96, 269
- Skrutskie, M. F., Cutri, R. M., Stiening, R., et al. 2006, *AJ*, 131, 1163
- Trundle, C., Dufton, P. L., Hunter, I., et al. 2007, *A&A*, 471, 625
- Udalski, A. 2000, *Acta Astron.*, 50, 279
- Udalski, A., Szymanski, M., Kubiak, M., et al. 1998, *Acta Astron.*, 48, 147
- Wallace, P. T., & Gray, N. 2003, *User's guide of ASTROM*
- Warren, Jr., W. H., & Hesser, J. E. 1977, *ApJS*, 34, 207
- Wisniewski, J. P., & Bjorkman, K. S. 2006, *ApJ*, 652, 458
- Wisniewski, J. P., Bjorkman, K. S., Bjorkman, J. E., & Clampin, M. 2007a, *ApJ*, 670, 1331
- Wisniewski, J. P., Bjorkman, K. S., Magalhães, A. M., et al. 2007b, *ApJ*, 671, 2040
- Wolff, S. C., Strom, S. E., Dror, D., & Venn, K. 2007, *AJ*, 133, 1092
- Zorec, J., & Frémat, Y. 2005, in *SF2A-2005: Semaine de l'Astrophysique Française*, ed. F. Casoli, T. Contini, J. M. Hameury, & L. Pagani, 361
- Zorec, J., Frémat, Y., & Cidale, L. 2005, *A&A*, 441, 235
- Zorec, J., Frémat, Y., Martayan, C., Cidale, L. S., & Torres, A. F. 2007, in *Active OB-Stars: Laboratories for Stellar and Circumstellar Physics*, ed. A. T. Okazaki, S. P. Owocki, & S. Stefl, ASP Conf. Ser., 361, 539